Mineralogy and Petrology (1993) 48: 309–341

Mineralogy and Petrology

Petrology and Geochemistry of Peridotites and Associated Vein Rocks of Zabargad Island, Red Sea, Egypt*

G. Kurat[1], H. Palme[2], A. Embey-Isztin[3], J. Touret[4], T. Ntaflos[5], B. Spettel[2], F. Brandstätter[1], C. Palme[2], G. Dreibus[2], and M. Prinz[6]

[1] Naturhistorisches Museum, Wien, Austria
[2] Max-Planck-Institut für Chemie, Mainz, Federal Republic of Germany
[3] Termeszettudomanyi Muzeum, Budapest, Hungary
[4] Instituut voor Aardwetenschappen, Vrije Universiteit, Amsterdam, The Netherlands
[5] Institut für Petrologie, Universität Wien, Austria
[6] Department of Mineral Sciences, American Museum of Natural History, New York, USA

With 12 Figures

Received December 11, 1992;
accepted March 31, 1993

Summary

Zabargad (St. John's) Island in the Red Sea contains three ultramafic bodies, one of which has produced the famous gem olivine (peridot). The ultramafic rock types consist of two major groups—the peridotites and the vein rocks within them. The peridotites are divided into three groups: primitive, depleted and metasomatized. The primitive peridotites are the most abundant and are represented by mainly pristine spinel-lherzolites which have chemical compositions representative of the subcontinental upper mantle. The depleted peridotites are mainly harzburgites and some dunites and both are similar to worldwide occurrences. The most depleted peridotites also appear to have the greatest metasomatic additions of incompatible elements, as has been noted at other localities. Metasomatic additions were clearly accompanied by tectonic shearing. Metasomatism included infiltration of incompatible elements and the formation of porphyroblasts of clinopyroxene, amphibole, Al-spinel and plagioclase; it took place under a variety of p-T conditions and with fluids of differing compositions.

The vein rocks are mainly monomineralic and comprise olivinites, orthopyroxenites, clinopyroxenites, websterites, hornblendites and plagioclasites. These rocks are believed to have formed from fluids similar to that which metasomatized the host rock, rather than by some kind of igneous process. The fluids were derived from peridotite reservoirs (fertile and depleted) and apparently were in equilibrium with these reservoirs. Highly abundant fluid inclusions document the hypersaline and CO_2-dominated character

* Dedicated to Prof. Josef Zemann on the occasion of his 70th birthday

of these fluids. Monomineralic vein rocks are closely associated with metasomatic and tectonic processes, and there is a complete transition between metasomatic impregnation and formation of vein rocks. These processes may have also been active in other peridotite bodies of the world, as was earlier recognized and documented in the Sciad Ultramafic Complex, California. Metasomatism is evident along clinopyroxenite and hornblendite veins, whereas orthopyroxenites, olivinites and plagioclasites do not show any interaction with the wall rocks. Olivinites are probably the latest (lowest p-T) vein rock type, and the latest olivine which formed within their open cavities became the gem peridot.

Zabargad ultramafic rocks preserve relic phases indicating an initial depth of origin greater than 85 km. Clinopyroxenites preserve the memories of the highest p-T conditions and they may be the first vein rock type formed in the peridotites. The p-T path of uplift coincides with the oceanic geotherm at great depth but deviates systematically from it with falling pressure in a series of tectonic stages accompanied by metasomatism and recrystallization. The p-T and petrologic history indicates rapid uplift, a feature which is supported by extensive contact metamorphism of the associated metasediments.

Zusammenfassung

Petrologie und Geochemie der Peridotite und der mit diesen vergesellschafteten Ganggesteine der Insel Zabargad, Rotes Meer, Ägypten

Auf der Insel Zabargad (St.John's Island) im Roten Meer befinden sich drei Peridotit-Körper von denen einer seit Jahrtausenden den berühmten Peridot (Edelolivin) geliefert hat. Die ultramafischen Gesteine von Zabargad gliedern sich in zwei Hauptgruppen: die Peridotite und die mit diesen vergesellschafteten Ganggesteine. Die Peridotite können in drei Gruppen gegliedert werden: die primitiven, die verarmten und die metasomatisch veränderten Peridotite. Am meisten verbreitet auf Zabargad sind die primitiven Peridotite. Diese sind meist Spinell-Lherzolithe mit einer chemischen Zusammensetzung, welche dem subkontinentalen Oberen Erdmantel entspricht. Die verarmten Peridotite werden hauptsächlich von Harzburgiten und einigen wenigen Duniten repräsentiert. Beide sind jenen aus anderen Vorkommen der Welt sehr ähnlich. Die am stärksten verarmten Peridotite scheinen auch die stärksten metasomatischen Veränderungen erfahren zu haben — ein Trend, der auch schon an anderen ultramafischen Komplexen erkannt wurde. Metasomatische Anreicherungen inkompatibler Spurenelemente sind häufig direkt mit tektonischer Verformung und Kataklase gekoppelt. Die Metasomatose ist als Infiltration inkompatibler Elemente erkennbar und führte auch zur Bildung von Porphyroblasten von Klinopyroxen, Amphibol, Al-Spinell und Plagioklas. Diese Bildungen fanden unter verschiedenen p-T-Bedingungen statt und erfolgten durch Fluide mit unterschiedlichen Zusammensetzungen.

Die (meist ultramafischen) Ganggesteine sind häufig monomineralisch und umfassen Olivinite, Orthopyroxenite, Klinopyroxenite, Websterite, Hornblendite und Plagioklasite. Wir glauben, daß diese Gesteine von Fluiden gebildet wurden, welche ähnlich jenen waren, die die Metasomatosen der Peridotite verursachten. Diese Genese wird von uns der magmatischen vorgezogen. Die Fluide stammten aus peridotitischen Reservoiren (fertilen und verarmten) und waren mit diesen offenbar im Gleichgewicht. Die Ganggesteine sind sehr reich an "fluid inclusions", welche allerdings keine Flüssigkeit enthalten, sondern nur Festkörper (Salze) und CO_2 ($\pm N_2$), also einen trockenen, hypersalinen Charakter haben. Auch die monomineralischen Ganggesteine sind eng mit tektonischen Prozessen verknüpft und somit auch mit metasomatischen Prozessen. Es existieren vollkommene Übergänge von metasomatischen Imprägnationen bis zu echten Ganggesteinen. Solche Prozesse waren offensichtlich auch weltweit in anderen

ultramafischen Komplexen aktiv und wurden schon im Seiad Ultramafic Complex in Kalifornien erkannt und beschrieben. Metasomatismus begleitet überlicherweise die Klinopyroxenit- und Hornblendit-Gänge. Orthopyroxenite, Olivinite und auch Plagioklasite zeigen jedoch keine Wechselwirkung mit den Wirtgesteinen. Olivinite sind wahrscheinlich die zuletzt gebildeten Ganggesteine. Der zuletzt sich bildende Olivin wurde der schönste und zum gesuchten Peridot.

Alle ultramafischen Gesteine von Zabargad enthalten Minerale aus verschiedenen Bildungsepochen. Einige Relikte erinnern an eine Herkunft aus einer Tiefe von mehr als 85 km. Klinopyroxenite konservierten die höchsten p-T-Bedingungen. Sie waren daher wahrscheinlich die ersten (noch erhaltenen) Ganggesteine, welche sich im peridotitischen Erdmantel unterhalb des heutigen Roten Meeres bildeten. Der p-T-Pfad der Zabargad Ultramafitite deckt sich in großer Tiefe mit der ozeanischen Geotherme. Mit abnehmender Tiefe entfernt sich dieser Pfad allerdings zunehmend von der Geotherme und läßt eine Reihe von tektonischen Aktivitäten verbunden mit Metasomatose und Rekristallisation erkennen. Die p-T-Geschichte der Zabargad Ultramafitite deuten auf einen raschen Aufstieg aus dem Erdmantel hin. Diese Daten werden durch die weitverbreitete und intensive Kontaktmetamorphose der mit den Peridotiten assoziierten Metasedimenten unterstützt.

Introduction

Zabargad (St. John's) Island is located near the central trough of the northern Red Sea at about 23°36,5'N, 36°12'E, approximately 55 km southeast of Ras Banas, Egypt. It is a small island which apparently represents an uplifted portion of the Red Sea lithosphere exposing peridotites, crustal basement rocks, and hornfelsic sediments (*Moon*, 1923, 1925; *Bonatti* et al., 1981, 1983, 1986; *Kurat* et al., 1982 a, b). Thus, Zabargad Island provides a unique opportunity to study in detail the upper mantle underlying the Red Sea.

Little was known about the Island before the 1980's, largely because of military restrictions. *Moon* (1923) in his first brief geological study, reported blocks of ultramafic rocks which intruded sediments and were subsequently uplifted above sea level. The short petrographic description of Moon's collection (*Moon*, 1925) and a small suite of rocks at the Naturhistorisches Museum in Vienna, collected during an expedition of S. M. Schiff "Pola" of the Austrian-Hungarian Navy in 1895 (*Pott*, 1898) testified to the presence of a variety of ultramafic rocks. They are accompanied by metamorphic rocks and by Quaternary basalts (*El Shazly* and *Saleeb*, 1972, 1979; *El Shazly* et al., 1974). Zabargad Island is also famous for its gem peridot which has been mined for several millennia, and after which it was named.

When military restrictions were loosened, we were able to visit Zabargad Island early in 1980 and sample the ultramafic rocks, basalts, and hornfelsic sediments. Since then, small preliminary reports on different aspects of our studies have been published (*Kurat* et al., 1982a, b, 1983, 1984, 1985, 1991b; *Ntaflos* et al., 1984; *Oberli* et al., 1987; *Zipfel* et al., 1991), as well as larger contributions by other research groups (*Clocchiatti* et al., 1981; *Bonatti* et al., 1981, 1983, 1986; *Styles* and *Gerdes*, 1983; *Nicolas* et al., 1985, 1987; *Brueckner* et al., 1988; *Petrini* et al., 1987; *Piccardo* et al., 1988). Here we present a detailed report of our studies on the ultramafic and related rocks of Zabargad Island.

This contribution is intended not only to widen the existing data base on Zabargad Island but also to introduce some petrogenetic models which differ from

previous ones. In addition, we make an attempt to unravel the geological history of the island by utilizing all data available at this time.

Tectonic Setting and Geology

Zabargad Island is situated at the western edge of the axial trough of the northern Red Sea. Its location is at the boundary between the zone of plate separation by seafloor spreading in the south, and the zone of extension by lithospheric attenuation in the north (*Girdler* and *Styles*, 1974; *Styles* and *Gerdes*, 1983; *Nicolas* et al., 1987). A large gravity anomaly (164 mgal) and magnetic anomalies are present over the island (*Triulzi*, 1898) indicating the presence of fresh peridotites to a depth of at least 8 km (*Styles* and *Gerdes*, 1983).

The island has an approximately triangular shape (Fig. 1) with about 3 km length of each side. It has a rough morphology reaching 250 m above sea level at the main peridotite hill. Approximately one third of the island's surface is covered by alluvium, older and young reefs, and evaporites. The exposed rocks consist of peridotites, metamorphic rocks, metasediments, and basalts. Three bodies of peridotites are present: the main peridotite hill (MPH), central peridotite hill (CPH), and northern peridotite hill (NPH) (terminology after *Moon*, 1923). Their contacts with metasediments and metamorphic rocks appear to be exclusively tectonic (see also *Nicolas* et al., 1987). The main masses of these bodies are made up of

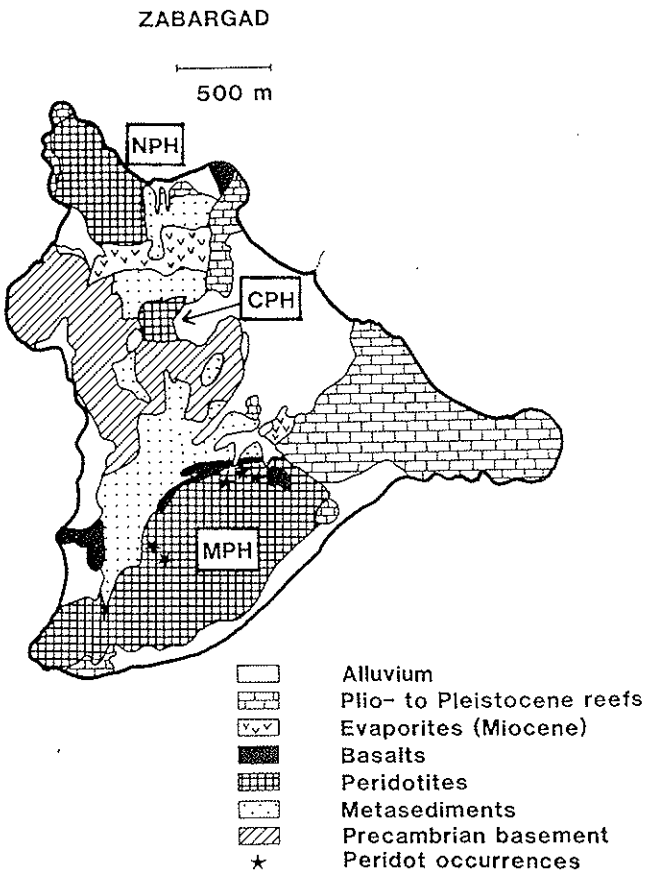

Fig. 1. Generalized map of Zabargad Island, Red Sea, Egypt (after *Moon*, 1923; *Bonatti* et al., 1981 and *Kurat* et al., 1982b)

spinel lherzolites with minor amounts of harzburgites, dunites, and plagioclase and amphibole-bearing rocks. All rocks are fresh and only small-scale serpentinization has been observed at the MPH, mainly associated with fracture zones containing the peridot-bearing olivinite vein rocks. The peridotites are occasionally cut by veinlets or veins of orthopyroxenites, clinopyroxenites, hornblendites and plagioclasites, in addition to olivinites. Basalt dikes are fairly abundant at the MPH. The ultramafic assemblages of the peridotites and vein rocks are described in detail below.

The metamorphic rocks consist of gneisses which are crisscrossed by amphibolite veins. They strongly resemble the metamorphic rocks of the Nubian Precambrian basement. *Boudier* et al. (1988) and *Seyler* and *Bonatti* (1988) showed that they are of deep crustal origin. The metasediments are hornfelses of former sediments which consisted of interlayers of limestones, siliceous limestones, carbonaceous shales, evaporites, and clastic sediments ("Zabargad Formation" according to *Bonatti* et al., 1981). They are highly metamorphosed and often rich in alkaline glass. Typical main mineral associations are: calcite, calcite + dolomite, dolomite, dolomite + phlogopite, quartz, quartz + scapolite, quartz + phlogopite, quartz + albite + phlogopite, quartz + scapolite + tremolite, tremolite, tremolite + scapolite, tremolite + phlogopite, and albite. Common minor minerals are plagioclase (oligoclase), talc, magnesite, gypsum, cordierite, Mg-chlorite, sulfides and Fe-oxides. The parent sediments may have been similar to the Mukawwar Formation (Cretaceous?) described by *Carella* and *Scarpa* (1962). Since there is no extensive magmatic activity on Zabargad Island, the high grade contact metamorphism is attributed to the hot intrusion of peridotite bodies into the sediments (*Moon*, 1925; *Kurat* et al., 1982 a, b; *Nicolas* et al., 1987).

Basalts are present in several small extrusives but mainly fill fissures in the peridotites and metasediments (*Petrini* et al., 1988). Within fissures and layers, evidence for small scale gravitational fractionation is omnipresent. Rock types range from basalt through plagiophyric dolerite to plagioclase-rich cumulates. Basalt flows, sometimes giving evidence of coming directly from fissures, develop pillow structures, indicating extrusion under water. The age of the basalts has been determined to be between 0.9–1.7 m.a. (*El Shazly* et al., 1974) in accordance with their geological position which is indicative of a late event.

Analytical Methods

Bulk compositions of selected samples were determined utilizing a variety of methods. Depending on average grain size, 5–10 g of each sample were homogenized and aliquots taken for analysis. Major element contents were determined by X-ray fluorescence analysis (XRFA). Glass disks, made of 1 g of sample and 5 g of $Li_2B_4O_4$, were analyzed against U.S.G.S. standard rocks utilizing a Philips 1400 spectrometer equipped with a Rh tube which was operated at 50 kV and 30 mA. Accuracy for the elements determined in this manner is estimated to be generally better than 5%.

Some major (Fe, Ca), minor, and many trace elements were determined by instrumental neutron activation analysis (INAA). About 200 mg of each sample were irradiated for 6 hours in a TRIGA MARK IV reactor at a neutron fluence of 7×10^{11} n/cm^2 sec. At various times after the end of neutron bombardment the activity of the samples was counted on Ge(Li) detectors. Spectra processing was done

according to the procedure of *Kruse* (1979). Appropriate element standards were included in the irradiations.

To determine the halogens, pulverized samples of 100–200 mg were irradiated with thermal neutrons for 2 hours. The irradiated samples were mixed with V_2O_5 and pyrohydrolysis was applied for the separation of the halogens (*Dreibus* et al., 1979). The extracted halogens were collected in a 5% NaOH solution and then divided into two parts. One part was used for the γ-counting of ^{38}Cl and ^{82}Br followed by the native F-measurements with a specific fluoride electrode. In the second part, ^{128}I was separated from the other halogens after addition of a γ-tracer with a CCl_4-extraction and was measured with a Ge(Li) well type detector.

The results of the major, minor and trace element determinations are presented in Tables 2, 3, 4, and 5. The CaO and FeO contents determined by INAA are not listed, but there is excellent agreement between XRFA and INAA data. The Cr, Mn, and Ni contents in Table 3 are those determined by INAA. Again, the XRFA data for these elements agree within a few percent with the INAA data.

Mineral analyses were carried out using an ARL-SEMQ electron microprobe. Wet chemically analyzed minerals were used as standards and correction procedures following *Bence* and *Albee* (1968) and *Albee* and *Ray* (1970) were applied. Mineral compositions are being published in a special publication of the Mineralogisch-Petrographische Abteilung, Naturhistorisches Museum Wien, and can be obtained from the first author.

Petrography

In this section only a short and general characterization of the main rock types is given (compare also Table 1). A more detailed description of the analyzed samples can be found in the special publication which contains also the mineral chemical data (see above).

Spinel lherzolite is the main component of the ultramafic rock types on Zabargad Island. It is characterized by an exceptional freshness, manifested in a lack of serpentine minerals in almost all of the samples. Another exceptional feature is the high proportion of rocks with a relatively high modal clinopyroxene content which may indicate that primitive (undepleted) lherzolites are unusually abundant on the island (see also *Piccardo* et al., 1988; *Kurat* et al., 1984; *Kurat*, 1991, 1992). In addition to the four common phases of spinel lherzolites, plagioclase is present in trace amounts in some of the samples, typically enveloping spinel crystals (see also *Bonatti* et al., 1986). Another phase present in small amounts in some samples is a brown amphibole generally found in the proximity of clinopyroxene and spinel.

The textures of the spinel lherzolites are mostly porphyroclastic (terminology follows *Mercier* and *Nicolas*, 1975), but protogranular-porphyroclastic transitional textures are also common. The large (>1 mm) porphyroclasts are olivine and orthopyroxene, while the smaller (<1 mm) crystals are mostly clinopyroxene and spinel. Porphyroclasts may occasionally be elongated and strained, and undulatory extinction and kink bands were found in some large olivine crystals. Rarely, highly deformed cataclastic textures also occur. These mylonitic textures, however, are confined to the summit area of the MPH. A remarkable feature of the Zabargad peridotites is that the texture, i.e., the degree of deformation, can change abruptly within a sample. A good example is sample Z-17 (see also Figs. 2C and 2D) which

Table 1. *Summary of sample rock types and provenance of peridotites and vein rocks from Zabargad Island*

Rock type	MPH	CPH	NPH	BW
Peridotites				
Sp-lherzolite	Z-13A			Z-118H
Sp-harzburgite		Z-103H		
Sp-plag-lherzolite	Z-14, Z-51	Z-34		
Sp-plag-harzburgite	Z-30			
Plag-amph-lherzolite	Z-106			
Amph-harzburgite	Z-15		Z-17D, Z-17G, Z-19	
Amph-dunite			Z-36	
Plag-wherlite	Z-26			
Vein Rocks				
Olivinite	Z-104			
Orthopyroxenite		Z-31		
Clinopyroxenite		Z-102, Z-103G		
Hornblendite	Z-28			
Plagioclasite	Z-13G			
Sp-websterite	Z-109			
Ol-plag-websterite	Z-52			
Plag-websterite				Z-118G
Plag-clinopyroxenite	Z-37			

Apparent abundances have no statistical significance.
MPH Main Peridotite Hill; *CPH* Central Peridotite Hill;
NPH Northern Peridotite Hill; *BW* Breakwater

also has impressive geochemical properties (see below). Less abundant lithologies include spinel harzburgites, plagioclase peridotites, amphibole peridotites and wehrlites as well as vein rocks such as olivinites, orthopyroxenites, clinopyroxenites, hornblendites, plagioclasites and websterites.

The vein rocks always have very coarse-grained pegmatoidal textures (Fig. 3). Grain sizes are usually in the cm range. Olivinites and hornblendites can contain crystals in the dm range and one orthopyroxenite (Z-31) contained crystals up to 1 m in diameter. The width of the veins ranges from a few mm to approximately 1 m. Textures range from equigranular (some websterites) to porphyroclastic (most pyroxenites) to highly complex cataclastic exhibiting several recrystallization events.

Results

The Peridiotites

Mineralogical, petrological and chemical investigations show that Zabargad peridotitic rocks may be divided into three groups: (1) primitive peridotites (i.e., rich in magmatophile elements such as Al, Ca and Na), (2) depleted peridotites, and (3) metasomatized peridotites.

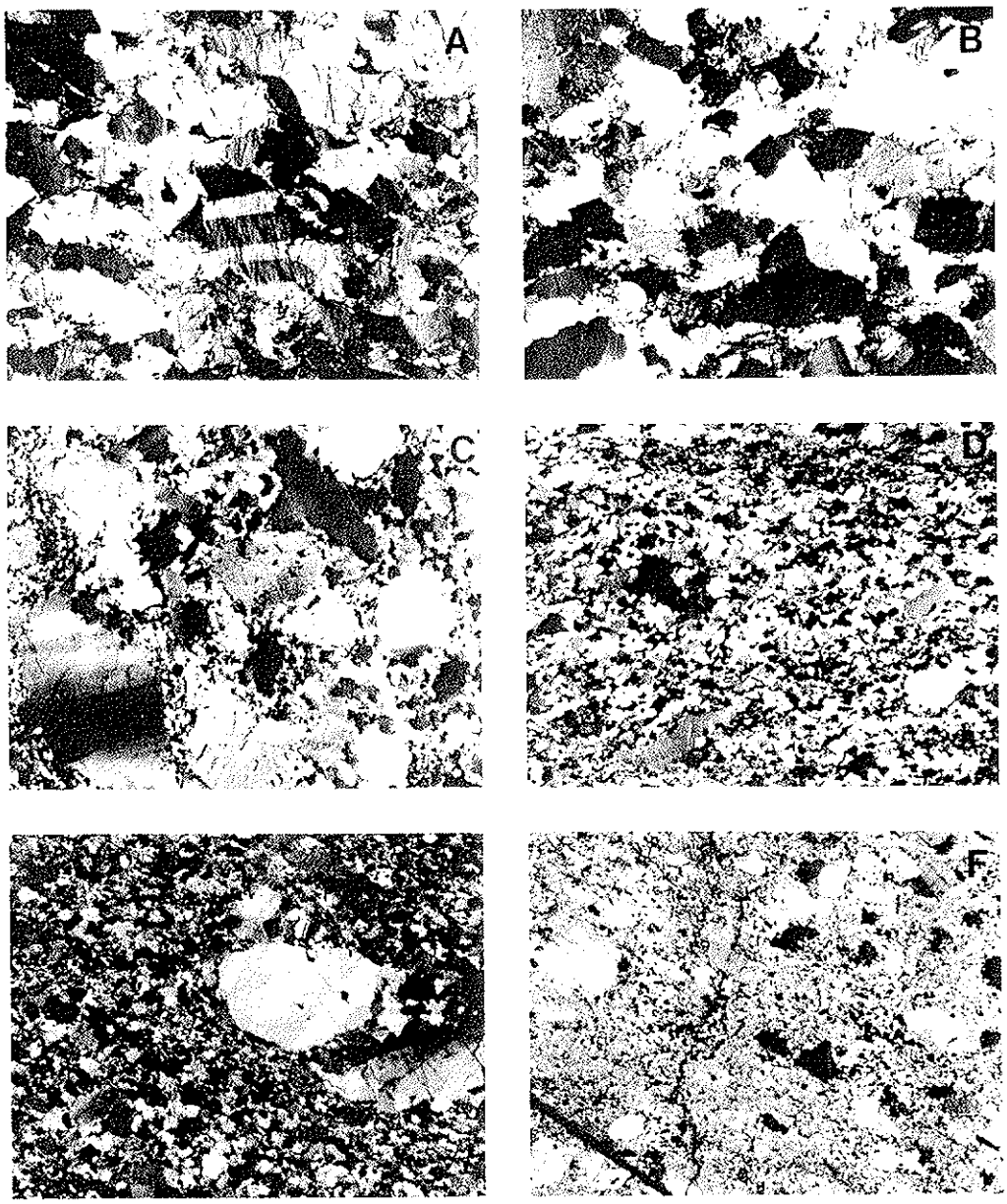

Fig. 2. Textures of peridotites from Zabargad Island. All photos are to the same scale with 11 mm width, and all were taken with xN. A: Primitive sp-lherzolite Z-118H. B: Primitive sp-plag-lherzolite Z-34. C: Amph-harzburgite Z-17G. D: Amph-harzburgite Z-17D. E: Amph-dunite Z-22. F: Plag-amph-lherzolite-mylonite Z-106, porphyroclastic portion

(1) *Primitive Peridotites*

This is the major ultramafic rock type of Zabargad Island represented here by our samples Z-13A, Z-14 and Z-106 from the MPH, Z-34 from the CPH and Z-118H, collected at the breakwater (probably belongs to the CPH). The most fertile rocks, spinel lherzolite Z-118H, spinel-plagioclase lherzolites Z-14 and Z-34, and plagioclase-amphibole lherzolite Z-106 have major and trace element

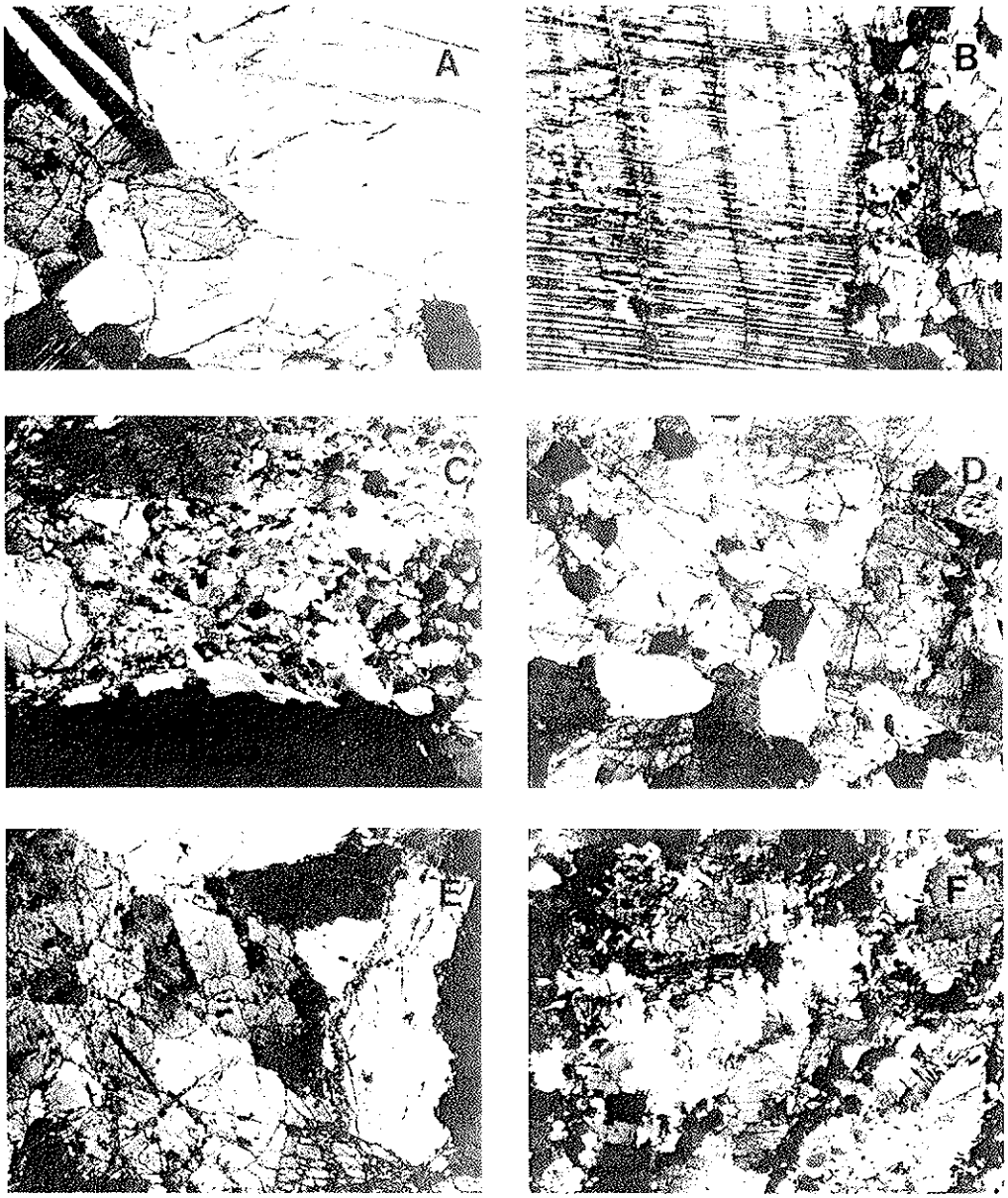

Fig. 3. Textures of vein rocks of Zabargad Island. All photos are at the same scale with 11 mm width, and all were taken with xN. A: Orthopyroxenite Z-31. B: Clinopyroxenite Z-102. C: Plag-clinopyroxenite Z-37 with large sp porphyroblast (black) and abundant plag. D: Sp-websterite Z-109. E: Hornblendite Z-28. F: Plagioclasite Z-13G

compositions (Tables 2, 3) which closely approach the estimated upper mantle composition (*Jagoutz* et al., 1979; *Palme* and *Nickel*, 1985). The rare earth element (REE) patterns are flat at about 2 × CI, or only slightly depleted for the light rare earth elements (LREE) (Fig. 6A). Spinel lherzolite Z-13A is, however, somewhat depleted, with ~1.4 × CI heavy rare earth elements (HREE) and ~1 × CI LREE (see Fig. 8B).

Table 2. *Major element contents of peridotites and associated vein rocks of Zabargad Island, Red Sea, Egypt, in wt.% (XRFA)*

	Peridotites											Vein Rocks						
Sample: Rock Local.	Z-13A Sp-lherz MPH	Z-14 Sp-plag-lherz MPH	Z-17G Amph-harzb NPH	Z-17D Amph-harzb NPH	Z-19 Amph-harzb NPH	Z-26 Plag-wehrl MPH	Z-34 Sp-plag-lherz CPH	Z-36 Amph-dunite NPH	Z-103H Sp-harzb CPH	Z-106 Plag-amph-lh MPH	Z-118H Sp-lherz	Z-13G Plag MPH	Z-28 Hornbl MPH	Z-31 Ortho pyrox CPH	Z-37 Plag-clinop MPH	Z-102 Clino pyrox CPH	Z-103G Clino pyrox CPH	Z-109 Sp-webst MPH
SiO_2	43.74	43.80	42.70	40.80	43.52	46.60	43.91	41.99	43.22	45.12	43.97	47.78	40.61	52.64	47.34	50.49	48.08	50.64
TiO_2	0.08	0.09	0.02	0.03	<0.02	0.38	0.14	0.06	0.06	0.11	0.15	0.30	0.32	0.19	0.46	0.17	0.11	0.44
Al_2O_3	2.44	3.06	0.58	0.94	1.43	5.86	3.64	1.53	1.18	2.85	3.56	18.11	10.68	5.17	10.44	6.24	11.96	5.98
FeO*	8.46	8.02	7.87	8.37	8.23	6.48	7.64	8.50	8.33	7.51	8.54	3.08	4.01	6.12	4.06	4.36	3.15	4.26
MgO	40.08	40.00	44.17	43.98	43.03	23.46	38.24	41.92	44.19	38.94	38.65	14.24	20.77	31.12	18.90	21.36	17.13	19.82
CaO	2.14	2.01	0.21	1.81	1.08	13.10	3.09	3.39	0.98	2.98	2.98	12.18	17.68	2.31	15.30	12.06	17.34	15.51
Na_2O	0.09	0.29	0.04	0.19	0.13	0.32	0.32	0.27	0.09	0.32	0.10	1.80	1.88	0.17	0.88	0.99	0.82	0.83
P_2O_5	<0.02	<0.02	<0.02	0.64	<0.02	0.02	<0.02	0.68	<0.02	<0.02	0.02	<0.02	0.03	<0.02	<0.02	0.04	<0.02	0.02
Total	97.03	97.27	95.59	96.76	97.42	96.22	96.98	98.34	98.05	97.83	97.97	97.49	95.98	97.12	97.38	95.71	98.59	97.50
100XMg	89.41	89.89	91.43	90.35	90.31	86.58	89.92	89.78	90.43	90.23	88.97	89.18	90.23	90.06	89.24	89.72	90.65	89.24

* Total Fe as FeO

Table 3. *Trace element contents of peridotites and vein rocks from Zabargad Island, Red Sea, Egypt. All data in ppm (INAA)*

	Peridotites												Vein Rocks						
	Z-13A Sp-lherz	Z-14 Sp-pl-lherz	Z-15 Amph-harzb	Z-17D Amph-harzb	Z-17G Amph-harzb	Z-19 Amph-harzb	Z-26 Plag-wehrl	Z-34 Sp-pl-lherz	Z-36 Amph-dunite	Z-103H Sp-harzb	Z-106 Pl-amph-lherz	Z-118H Sp-lherz	Z-13G Plagio-clasite	Z-31 Ortho-pyrox	Z-102 Clino-pyrox	Z-103G Clino-pyrox	Z-104 Olivi-nite	Z-109 Sp-webster	Accuracy %
Cl		605	150	960	230	390	840	515	970	335	660	360	180		1240	560	2170	1760	15
K	103	140	65	220	110	125	146	206	545	28	210	140	1430	92	275	51	88	715	10
Sc	13.8	16.1	12.0	8.35	5.26	9.87	54.1	15.3	10.9	9.55	17.7	14.6	22.2	18.5	31.2	51.3	2.65	43.9	3
Cr	2280	2528	3520	3095	2550	2450	1790	2480	2600	2210	2590	2400	722	3760	7870	4380	1.51	7340	3
Mn	1064	950	890	1030	1030	990	1197	975	1130	1090	870	1075	428	995	833	684	910	710	3
Co	112	106	105	112	119	110	61.1	108	97.8	121	99.7	111	40	69.4	36.5	47.1	144	33.8	3
Ni	2130	2265	2280	2390	2750	2474	1020	2220	2390	2600	2085	2320	1010	1130	610	970	4100	580	5
Zn	50	56	60	47	48	72		72	38	53	56	68	37	53	90	58	32		15
Ga	2.4	2.8	2.2	1.1		1.2	6.54	3.23	1.26	1.6	3.47	3.84	10.8	4.12	4.68	5.16		5.36	10
Br		0.35		0.21	0.17	0.14	1.96	0.55	0.65	0.43		1.08		0.24	0.64	0.92	2.1	1.1	15
La	0.23	0.21	0.084	5.93	0.5	0.67	0.5	0.19	13.8	0.03	0.33	0.43	1.96	0.085	0.67	0.18	0.11	2.48	5
Ce	0.59	0.68		13.9	0.98	1.16	2.35	0.86	34.8	0.073	0.83	1.2	4.42	0.3	1.8		0.17	6.46	10
Nd	0.53	0.60		7.45	0.47	0.41	2.5	0.64	19.6			0.9	2.87	0.28	2			6.13	20
Sm	0.18	0.21	0.101	1.8	0.113	0.064	1.06	0.252	4	0.015	0.234	0.3	0.85	0.118	0.73	0.155	0.005	1.66	4
Eu	0.066	0.083	0.052	0.393	0.027	0.022	0.398	0.104	0.774	0.011	0.092	0.117	0.44	0.052	0.294	0.076		0.547	5
Gd				1.7			1.1		3				0.95		1				25
Tb	0.057	0.075		0.24			0.27	0.075	0.42		0.068	0.08	0.16	0.05	0.2	0.1		0.26	10
Dy	0.38	0.54		1.3		0.08	1.85	0.59	2.25			0.57	1.12	0.39	1.35	0.84		1.59	10
Ho	0.083	0.13		0.24			0.42	0.13	0.44		0.12	0.13	0.26	0.093	0.31	0.23		0.3	15
Tm	0.032						0.23		0.11			0.057	0.079		0.13	0.14		0.16	15
Yb	0.25	0.34	0.23	0.37	0.041	0.045	1.16	0.38	0.57	0.14	0.39	0.36	0.52	0.33	0.77	1.03	0.015	0.73	10
Lu	0.034	0.057	0.037	0.043	0.006	0.009	0.173	0.059	0.07	0.025	0.06	0.054	0.078	0.051	0.117	0.156	0.007	0.124	5
Hf	0.11	0.10		0.18			0.46	0.15		0.034	0.13	0.18	0.38	0.12	0.29	0.06		0.63	10
Ta	0.007			0.49					0.17				0.035	0.07					20
Ir	0.0056	0.0038	0.0054	0.0047	0.0055	0.0042	0.028	0.0041	0.0046		0.0045	0.003		0.0053			0.0009		15
Au	0.0014			0.002	0.0006		0.009		0.0011			0.0016	0.0003		0.0008		0.0004	0.0004	15
Th				1.61	0.23	0.22			1.42									0.13	10
U				0.1	0.023	0.05			0.17			0.065			0.075			0.16	15

Textures of the fertile peridotites are either protogranular-porphyroclastic (Z-118H) or porphyroclastic with evidence of recrystallization (Fig. 2). However, occasionally tectonization grading up to mylonitization (Z-106) is present.

Mineral compositions reflect the tectonic history. Olivines have Fo contents around 90 and are rather homogeneous. Orthopyroxenes display a complex pattern, and their compositions vary from Al-rich porphyroclasts to Al-poor neoblasts within the same rock sample (Fig. 4). The Al/Cr ratios of orthopyroxenes vary according to the Al/Cr ratios of the rock and the p-T conditions for the different recystallization events. A similar situation is found for the clinopyroxenes (Fig. 4).

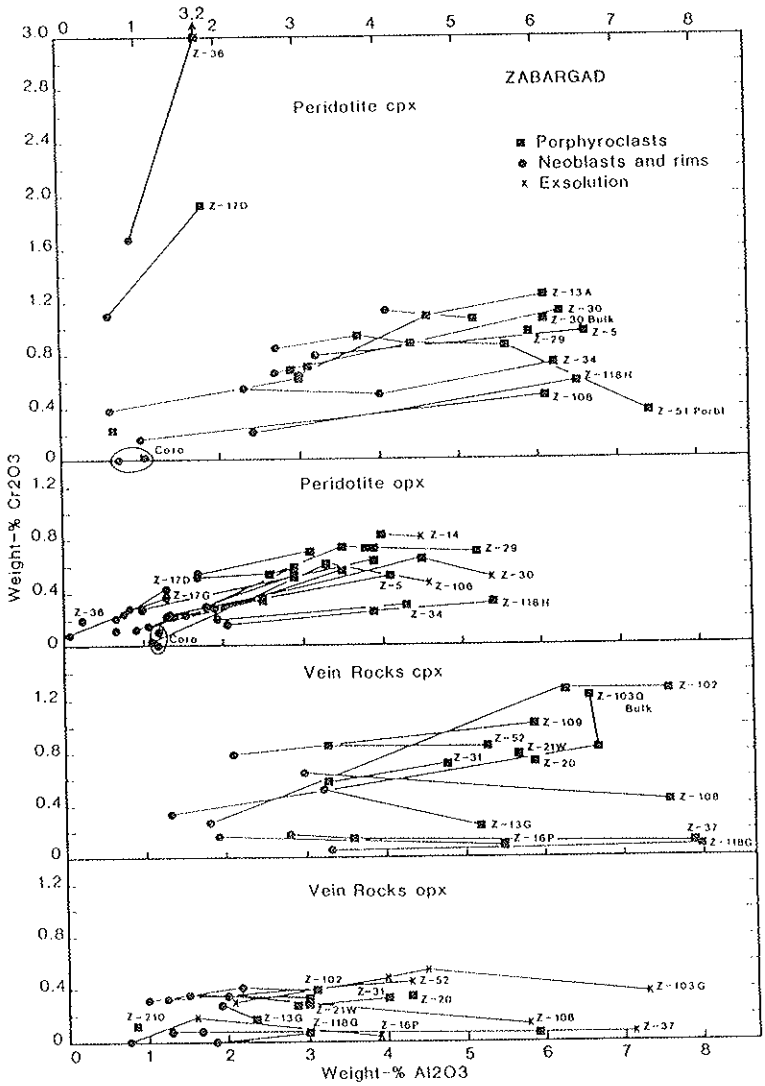

Fig. 4. Weight % Al_2O_3 vs. Cr_2O_3 for clinopyroxene and orthopyroxene of peridotites and vein rocks of Zabargad Island. Coexisting pyroxenes are connected by tie lines. Abbreviations: Porbl. = porphyroblast; Coro = corona pyroxene

Amphiboles are typical pargasitic hornblendes to pargasites which have fairly homogeneous compositions. However, Z-118H has two generations of amphibole; one is Ti- and Cr-rich, the other Ti- and Cr-poor.

Spinels have uniform compositions in plagioclase-free peridotites. In the most fertile samples they are typically poor in Cr_2O_3 (8.7 and 8.8% in Z-34 and Z-118H, respectively). Spinels develop thin rims which usually have 3–4% higher Cr_2O_3 contents than the original spinel in plagioclase-bearing rocks. Slightly depleted rocks of the primitive suite have spinels with higher Cr_2O_3 contents (14.1 for Z-14, 15.2 for Z-106). In addition to "normal" spinel Z-14 contains spinel porphyroblasts which have a completely different composition. They are extremely poor in Cr_2O_3 (2.6 wt%), apparently in disequilibrium with the rock.

The bulk rock composition (Table 2) has been slightly affected and has a somewhat disturbed Ca/Al ratio (Al-enriched).

(2) *Depleted Peridotites*

This group, much less voluminous than the preceding one, consists of harzburgites. Rocks for which trace element data are available (Z-15, Z-103H), are slightly depleted in HREE and more strongly in the LREE (Fig. 6A). Two rocks described below with the metasomatized peridotites, amphibole harzburgites Z-17G and Z-19 (Fig. 6B) are the most extremely depleted samples encountered. They, however, show some subsequent metasomatic enrichments in LREE. Textures are complex porphyroclastic, with strongly deformed porphyroclasts and usually with several generations of neoblasts.

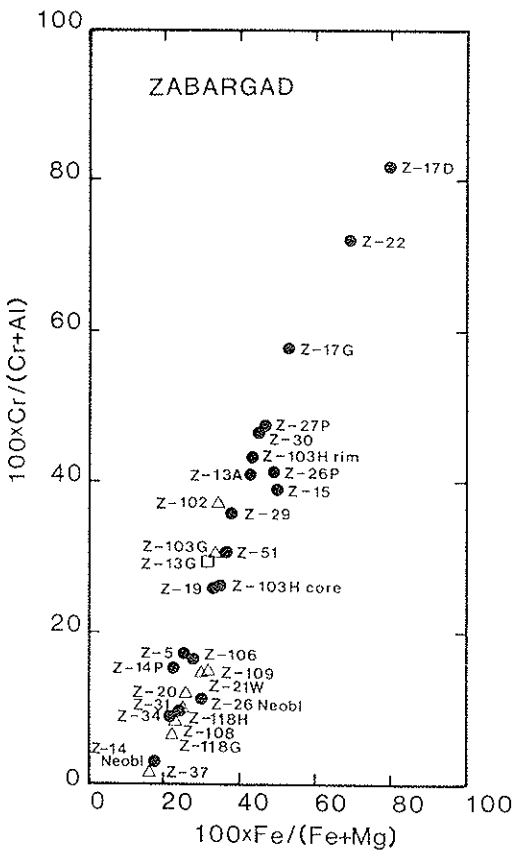

Fig. 5. Plot of atomic 100 × Fe/(Fe + Mg) vs. 100 × Cr/(Cr + Al) for spinels of the peridotites and vein rocks of Zabargad Island. Dots: peridotites; open symbols: Vein rocks. Numbers are sample numbers

Olivines have homogeneous compositions, $Fo_{90.3-91.0}$. Orthopyroxenes have highly variable compositions (Fig. 4). They range from highly aluminous (up to 5.2% Al_2O_3), with rather low Al/Cr ratios, to Al-poor compositions (down to 1% Al_2O_3) with decreasing Al/Cr ratio. In addition, we observed reaction rim coronas at plagioclase-olivine contacts in plagioclase-bearing peridotites with Al-poor and yet nearly Cr-free orthopyroxenes.

Clinopyroxenes have characteristics similar to that of orthopyroxenes. Porphyroclasts are Al-rich, neoblasts are poorer in Al, and corona clinopyroxenes are Cr-poor. Amphiboles are pargasitic hornblendes to pargasites. They are usually homogeneous but occasionally (see Z-15) two generations are present. Spinels in depleted peridotites are rich in Cr_2O_3 (23.1–36.1%) and slightly inhomogeneous, with rims enriched in Cr (e.g., Z-103H). Plagioclase is generally calcic, with An-contents above 80 (Appendix II). However, Z-15 also contains small amounts of plagioclase of An 30.

(3) *Metasomatized Peridotites*

A variety of peridotitic rocks were encountered which show evidence of modal metasomatic alteration by the growth of porphyroblasts of amphibole (Z-17D, Z-36) or clinopyroxene (Z-26, Z-51). These rocks are strongly enriched in incompatible trace elements and, at the same time, are depleted in magmatophile major

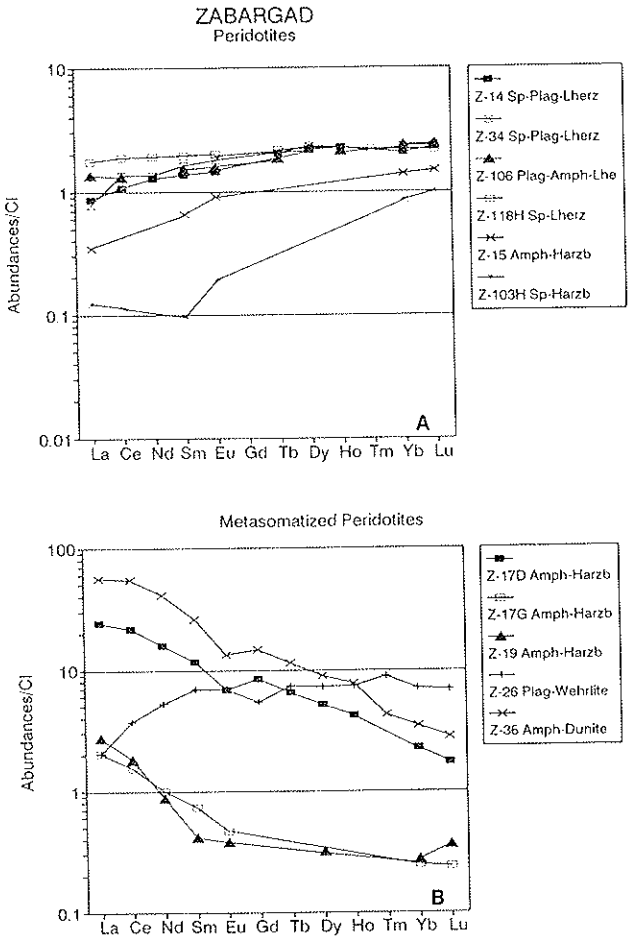

Fig. 6. Abundances of REEs in peridotites from Zabargad Island normalized to CI abundances (*Palme* et al., 1981). A: Primitive lherzolites and slightly depleted peridotites (harzburgites). B: Metasomatized peridotites. All samples are patently metasomatized, displaying neoblasts of amphibole or clinopyroxene. Note the different REE contents of samples Z-17D and Z-17G, the cataclased and porphyroclastic portions, respectively, of one sample (see Figs. 2C, D)

elements (Table 3). Those rocks with amphibole porphyroblasts show a steep REE pattern with LREE 22xCI and 55xCI, and HREE 2xCI and 3xCI for Z-17D and Z-36, respectively (Fig. 6B, see also Fig. 13 of *Bonatti* et al., 1986). However, it is clear that not all amphibole-bearing peridotites are enriched, e.g., both Z-15 and Z-106 (Fig. 6A) contain amphibole, but are strongly depleted in LREE (they therefore are classed with the depleted peridotites). Although much less affected than the patently metasomatized peridotites, amphibole harzburgites Z-17G and Z-19, in our opinion also belong to this group (terminology after *Dawson*, 1984). With respect to HREE and other magmatophilic elements these are the most depleted rocks encountered on Zabargad Island.

Textures of metasomatized peridotites are generally porphyroclastic to equilibrated and show the highest degree of recrystallization (Fig. 2D and 2E). Metasomatism appears to be related to texture, as exemplified by sample Z-17, which consists of highly deformed and recrystallized amphibole harzburgite Z-17D which is strongly enriched in incompatible trace elements, in contrast to

Table 4. *Trace element contents of minerals separated from peridotites and vein rocks from Zabargad Island (in ppm).* Cpx *clinopyroxene;* Amph *amphibole;* Ol *olivine*

	Cpx Z-15C	Cpx Z-26C	Cpx Z-103C	Amph Z-28C	Amph Z-36A	Ol Gem	Ol Z104O
Cl	340		1050	5000	950		
K	65	73	210	1850	4080		35
Sc	49.9	85.5	50.6	62.5	48.4	3.06	9.07
Cr	8800	2650	8510	7430	14060	12.6	93
Mn	682	1075	810	430	685	950	985
Co	26.2	32.9	28.2	28.4	36.9	123.6	130
Ni	360	520	470	707	860	2690	2820
Zn	41	110	44		100	34	36
Ga	4	8.26	4.53	7.06	7.5		
Br			1.5	3.02			0.33
La	0.19	0.71	0.41	5.82	13.6	0.004	0.039
Ce		3	1.3	16.5	64.1		
Nd	1.6	3.8		7.03	35.8		
Sm	0.72	1.56	0.57	1.78	8.22	0.0012	
Eu	0.318	0.56	0.24	0.906	2.7		
Gd				1.8	6.3		
Tb	0.26	0.48	0.24	0.32	1.11		
Dy	2.1	3	1.9	2.46	5.9		
Ho	0.5	0.67	0.46	0.57	1.2		
Tm				0.28			
Yb	1.57	1.91	1.2	1.56	1.93	0.019	0.042
Lu	0.23	0.29	0.21	0.246	0.23	0.0056	0.014
Hf	0.28	0.7	0.23	0.66			
Ta		0.11		0.053	1.83		
Ir		0.037	0.005				
Au		0.02	0.0089	0.0025			

the porphyroclastic amphibole harzburgite Z-17G with which it forms a compound sample.

Olivines have uniform compositions, with high Fo (91.0–91.6) in depleted samples (Z-17G, Z-17D and Z-19); others are $Fo_{90.2-90.5}$. Orthopyroxene compositions are complex and generally poor in Al (Fig. 4). Only two samples of this suite contain orthopyroxene porphyroclasts with Al_2O_3 contents above 3% (Z-26 and Z-51). Most orthopyroxene has recrystallized in different events and compositions extend down to 0.07% Al_2O_3 (Z-17G). Al/Cr ratios are low (in accordance with the depleted nature of the rocks) and extend down to an extreme of about one (Z-17G and Z-36). Clinopyroxene follows the same trend as orthopyroxene, except for Z-51 which has Al-rich porphyroclasts (5.6% Al_2O_3) and very Al-rich porphyroblasts (7.4% Al_2O_3) which apparently are in disequilibrium with the rock. Trace element contents of clinopyroxene porphyroblasts in Z-15 (Table 4, Fig. 7A) are typical for clinopyroxenes of relatively fertile peridoditic rocks (e.g., *Kurat* et al., 1980; *Stosch*, 1982). Amphiboles are pargasitic and are normally Ti-poor (Z-19, Z-36). Z-17G has three different amphiboles, originating apparently from different recrystallization and metasomatism events. Trace element contents of porphyroblasts in amphibole dunite Z-36 are high with the LREE enriched over the HREE (Table 4, Fig. 7A), similar to the bulk rock sample (Fig. 6B). Spinels are generally Cr-rich (22.2–51.1% Cr_2O_3). In

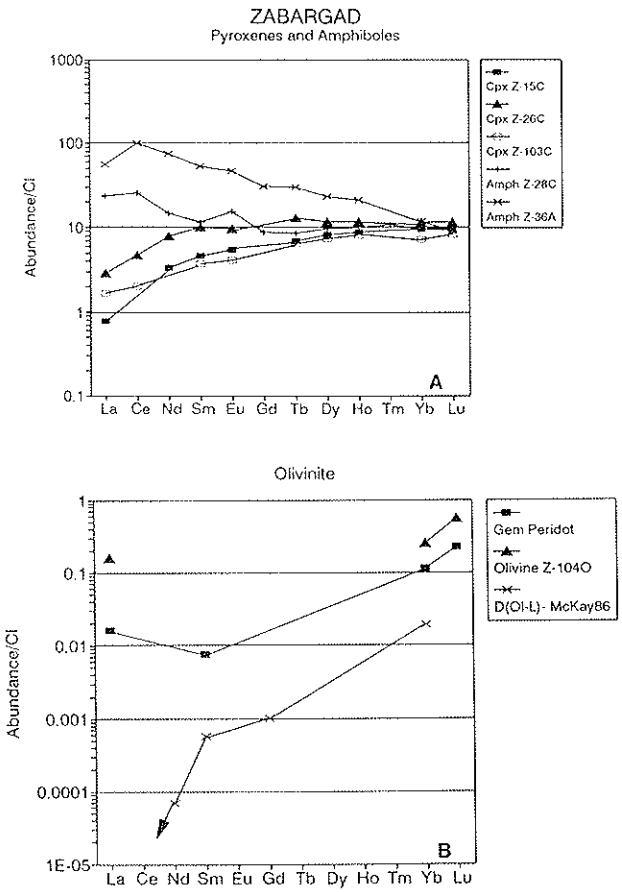

Fig. 7. Abundances of REEs in separated minerals from peridotites and vein rocks of Zabargad Island normalized to CI abundances (*Palme* et al., 1981). A: Clinopyroxenes and amphiboles. Z-15C: clinopyroxene porphyroblast in amph-harzburgite; Z-26C: clinopyroxene porphyroblast in plag-wehrlite; Z-103C: clinopyroxene from clinopyroxenite; Z-28C: amphibole from hornblendite; Z-36A: amphibole from amph-dunite. B: Brown vein olivine (Z-104O) and gem peridot from olivinites. Experimentally determined olivine-liquid distribution coefficients (*McKay*, 1986) are shown for comparison

addition, spinel porphyroblasts are present in Z-26 which are in disequilibrium with the rock, a feature also found in other samples; plagioclase is An 78.0–80.7.

The Vein Rocks

A variety of dikes and dikelets (mm to m in width) are present in the peridotites of Zabargad Island. They are either monomineralic or consist of only a few phases. The following types have been found: (1) olivinites, (2) orthopyroxenites, (3) clinopyroxenites, (4) websterites, (5) hornblendites, and (6) plagioclasites.

(1) *Olivinites* occur as dikes of m to dm dimensions, exclusively in the MPH, and are the parent rocks of the famous gem peridot. They consist of very large platy olivine crystals (up to 20 cm) of brown color, with some serpentine in the interstices. They have abundant open cavities which occasionally contain clean, clear crystals of green peridot. The large brown olivine crystals tend to become inclusion-poor and green in color at the margins, ending in these cavities. Olivine in the olivinites is compositionally almost indistinguishable from olivine in the peridotites (e.g., *Kurat* et al., 1982b). It has high Ni and Co contents and is low in incompatible trace elements (Tables 3, 4). There is a clear difference in trace element content (Table 4, Fig. 7B) between the green gem peridot and the fluid inclusion-rich brown olivine in the olivinite (Z-1040). However, both olivines are surprisingly rich in REEs if the very low distribution coefficients for these elements between olivine and liquid (*McKay*, 1986) are taken into account. The rock Z-104 is very rich in Cl and Br due to the presence of abundant hypersaline fluid inclusions (see Table 5 and discussion below).

(2) *Orthopyroxenites* are present as dikes, from cm to m wide, in all three peridotite hills of the island. Their grain size is very large, mostly in the cm range (5–10 cm). One dike, however, at the northern edge of MPH has orthopyroxene crystals up to one meter in diameter.

The bulk composition of Z-31 (Tables 2, 3) is typically that of a pyroxene-dominated rock, with high Sc, Cr, and Mn and low Co and Ni (but in the correct

Table 5. *Halogen contents of the sheared and granular portions of an amphibole harzburgite and a clinopyroxenite vein and host spinel harzburgite, compared to carbonaceous chondrite (CI) and seawater (in ppm)*

	Z-17D Amph-harzb Sheared	Z-17G Amph-harzb Granular	Z-103G Cpxite	Z-103H Sp-harzb	CI (1)	Seawater (2)
F	38 ± 4	6.0 ± 0.8	16 ± 2	16 ± 2	54	1.4
Cl	960 ± 40	230 ± 23	560 ± 30	330 ± 34	678	19350
Br	0.21 ± 0.02	0.17 ± 0.02	0.92 ± 0.08	0.43 ± 0.04	2.53	65
I	0.10 ± 0.01	0.059 ± 0.006	0.24 ± 0.02	0.24 ± 0.02	0.56	0.050
Cl/I	9600	3900	2300	1400	1200	387000
Br/I	2.1	2.9	3.8	1.8	4.5	1300

(1) *Palme* et al. (1981)
(2) Data from *Wedepohl* (1969)

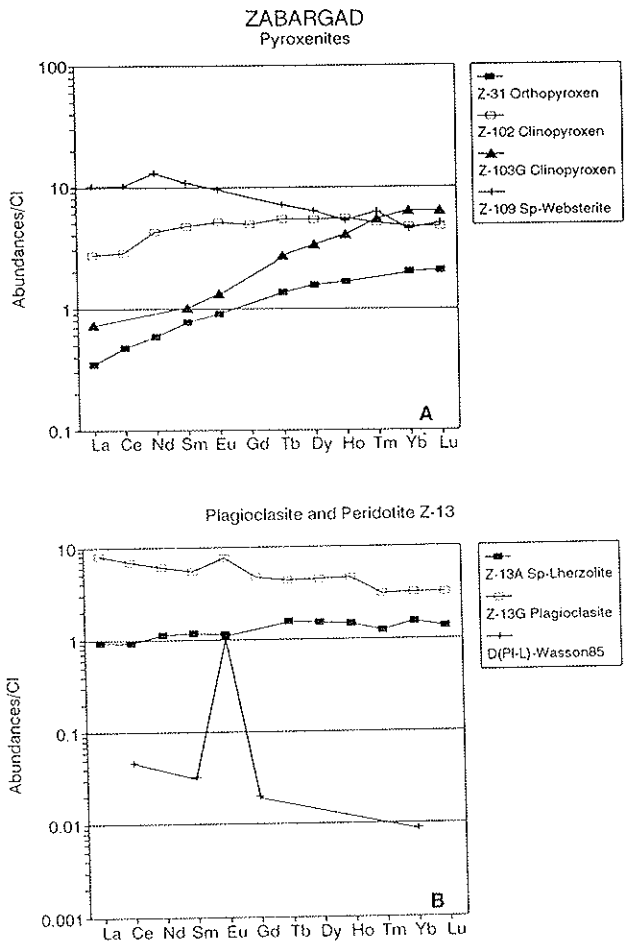

Fig. 8. Abundances of REEs in pyroxenites and a plagioclasite from Zabargad Island, normalized to CI abundances (*Palme* et al., 1981). A: Pyroxenites. B: Plagioclasite Z-13G and its host lherzolite Z-13A. Note the high contents of REEs in the plagioclasite despite the low crystal-liquid partition coefficients for plagioclase (e.g., *Wasson*, 1985)

proportion for an orthopyroxene in equilibrium with a peridotite, e.g., *Kurat* et al., 1980; *Stosch*, 1982). Abundances of the HREEs are at 2 × CI, but La is much less abundant (0.35 × CI) (Fig. 8A).

Mineral compositions in orthopyroxenites are similar to those in the peridotites. Olivine is Fo 91 and orthopyroxene in Z-31 (En 90.2) has an Al_2O_3 content comparable to orthopyroxenes in the peridotites, but with a higher Al/Cr ratio. Clinopyroxene in Z-31 is Al_2O_3-rich. Amphibole in Z-31 is particularly rich in Al_2O_3 and TiO_2, and spinel has a Cr_2O_3-poor (9.6%) primitive composition (Fig. 5).

(3) *Clinopyroxenites* occur in all three peridotite bodies on Zabargad Island but are particularly common on the CPH. They form dikelets and dikes of mm to m size. In places, dikelets form stringers of clinopyroxene porphyroblasts arranged parallel to the foliation of the host rock. In other places, the clinopyroxene porphyroblast stringers, dikelets and cm sized dikes run in swarms through the host rock, centimeters apart.

In spite of their similar mode of occurrence, clinopyroxenites have surprisingly different mineral and bulk compositions from one another. From a textural point of view two groups can be distinguished: one group of clinopyroxenites (represented by Z-102) has a thoroughly recrystallized matrix, shows some

growth of amphibole and has cloudy zones in the clinopyroxene porphyroclasts; the other group of samples (Z-37 and Z-103G) has clear porphyroclasts with bent exsolution lamellae and multiply tectonized and recrystallized matrices.

The first group of clinopyroxenites (Z-102) is characterized by high contents of Sc, Cr and REEs, and a very high content of Cl. (Table 3). The REE pattern (Fig. 8A) is fairly flat with 5 × CI HREE and slightly depleted LREE (~2.5 × CI). Mineral compositions are similar to those of peridotites. Clinopyroxene porphyroclasts are rich in Al_2O_3, Cr_2O_3 and Na_2O and neoblasts have successively lower contents (Fig. 4). Amphiboles are present in two generations. Spinel has 31.4% Cr_2O_3 and plagioclase has An 52.2.

Clinopyroxenites of the second group (Z-37 and Z-103G) have fairly different mineral compositions from one another. All samples have highly aluminous clinopyroxene porphyroclasts but are fairly poor in Na. They have different Cr_2O_3 contents (and therefore Al/Cr ratios) of 0.82 (Z-103G) and 0.10 wt.% (Z-37). Neoblasts have either about the same Al/Cr ratio (Z-103G) or a lower one. Spinel compositions are approximately in equilibrium with clinopyroxene compositions. Z-37 has, however, extremely low- Cr_2O_3 (1.44%) spinel porphyroblasts (similar to green spinel porphyroblasts in peridotites), whereas the spinel of Z-103G is Cr-rich (30.4%). The latter composition is similar to the composition of spinel rims in the host harzburgite (Z-103H). Plagioclase compositions range from An 63.3–82.7.

Trace element data for Z-103G show high contents of Cl, Sc, Cr and REE (Table 3). Data for a separated clinopyroxene porphyroclast (Z-103C in Table 4) show the same elements at an even higher level. The REE patterns for the rock and separated clinopyroxene are subparallel (Figs. 7A and 8A).

(4) *Websterites* are present in all of the peridotite bodies. They form veinlets and veins from cm to dm in width. Most of them have coarse-grained granular textures, except for Z-52 which is porphyroclastic and tectonically deformed. The granular websterites display different degrees of amphibolization, the least affected being Z-109. All websterites have clinopyroxenes and orthopyroxenes with abundant exsolution lamellae.

Based on clinopyroxene compositions, two groups of websterites can be distinguished: (a) a high-Cr group (Z-52, Z-109) and (b) a low-Cr group (Z-118G). Both have high Al contents.

(a) *High Cr Group*

Clinopyroxene has a composition comparable to that of clinopyroxene in fertile lherzolites. It has high TiO_2, Al_2O_3 and Na_2O but has slightly higher FeO than average clinopyroxene from peridotites. Neoblasts and rims show reequilibration at lower p-T conditions, as do the abundant exsolution lamellae. Orthopyroxene is either in equilibrium with clinopyroxene (Z-52), or represents various stages of recrystallization. Amphibole is typically rich in TiO_2, Al_2O_3, Cr_2O_3 and Na_2O with amphibole Z-109 being very rich in TiO_2 and Cr_2O_3. Spinels, when present, have fairly low Cr_2O_3 contents, comparable to slightly depleted lherzolites. Plagioclase is fairly sodic and also comparable to that in fertile lherzolite. Rare olivine has a composition similar to that of peridotite olivine. Trace element data for Z-109 (Table 3) are characterized by high contents of Cl, Sc, Cr and REEs. The REE pattern

(Fig. 8A) is fractionated with an increasing abundances from Lu (~4 × CI) to La (~10 × CI).

(b) *Low Ca Group*

Chemical compositions of minerals in Z-118G show that this rock is clearly out of equilibrium with the surrounding peridotites. Clinopyroxene (Fig. 4) has outstandingly high Al_2O_3 (8.0%), fairly high FeO (3.2%), but very low Cr_2O_3 (0.08%) contents. Orthopyroxene is apparently recrystallized (low Al_2O_3, in disequilibrium with the primary clinopyroxene), and has the same signature—very low Cr_2O_3 (0.06%) and high FeO (7.4%) contents. Olivine is Fo 88.8 and amphibole is rich in Al_2O_3 and FeO and poor in Cr_2O_3 (0.10%). Spinel is aluminous, but has minor elements typical of lherzolite spinels. Plagioclase is sodic (An 52.4) and comparable to fertile lherzolite plagioclase.

(5) *Hornblendites* are common on MPH and NPH. They occur either as isolated veins or dikes, or in swarms, or in the vicinity of orthopyroxenite dikes (Z-28). Their width commonly ranges from dm to m. They are coarse-grained to very coarse-grained, with crystal lengths reaching 10 cm or more. Compositions of the amphiboles are fairly uniform and do not show the diversity encountered in peridotites, pyroxenites and plagioclasites. They are fairly poor in TiO_2 and rich in Al_2O_3, Cr_2O_3 and Na_2O and always contain some K_2O and NiO; MnO contents tend to be low. Hornblendites, as do olivinites, show the most pronounced tendency towards being monomineralic. Rare relics of olivine can, however, be present and they have the typical composition of peridotitic olivine. Bulk major element contents are in accordance with the mineral compositions.

Trace element contents in amphibole (Table 4, Fig. 7A) are typically high. The REE pattern shows an enrichment of LREE over the HREE.

(6) *Plagioclasites* are abundantly present, mainly on MPH. In contrast to all other monomineralic vein rocks, they form bodies of restricted widths. Most commonly they are between 4 and 8 cm wide. They are always very coarse-grained and of nearly constant grain size (1–2 cm). Relic minerals from the host rock are always present, and amphibole and phlogopite may be present as neoblasts.

Plagioclase has a calcic composition (An 73–81), which is indistinguishable from the peridotite plagioclase. Porphyroclasts of olivine are common and have compositions similar to that of peridotite olivine, with a slight tendency towards lower Fo contents (88.8–89.5). Orthopyroxene follows the same trend, and is poor in Al_2O_3. Clinopyroxene has compositions which can be interpreted as evidence for reequilibration with the Cr-poor plagioclasite system. This implies that plagioclasites formed under conditions which did not allow Cr to be mobilized. However, TiO_2 contents are fairly high in clinopyroxene and even higher than that of clinopyroxene from fertile lherzolites. Amphibole compositions of the samples analyzed are highly diverse; all are Al_2O_3-rich, but differ considerably in their TiO_2, Cr_2O_3 and K_2O contents which could be either high or low. Spinel in Z-13G is fairly Cr_2O_3-rich (24.4%) and similar to the spinel of the host rock (Z-13A), in spite of the abundance of plagioclase.

Bulk compositions of plagioclasites (Tables 2.3) are typically depleted in compatible elements (Co, Ni, Cr) and surprisingly also in Cl. They are enriched in K, Sc, Ga and REE. The REE pattern (Fig. 8B) is only slightly fractionated, with Lu ~4 × CI and La 8 × CI and has a positive Eu anomaly. The REE

content is surprisingly high if the very low crystal-liquid partition coefficients are considered (e.g., *Irving*, 1978).

Fluid Inclusions in the Vein Rocks

Fluid inclusions have been studied in the most important vein rocks: olivinite (Z-104) and gem peridot of the MPH, orthopyroxenite (Z-31) and clinopyroxenite (Z-102) from the CPH.

(1) *Olivinite and Gem Peridot*

Gem peridot and brown olivine of olivinite (Z-104) have the same fluid inclusion compositions, but with highly different abundances. Brown olivines are richer in fluid inclusions. Typical primary inclusions (Fig. 9) are relatively large (up to 100 μm), isolated, and have very complex lobate shapes. They do not contain any fluid liquid at room temperature (no visible trace of water), but have a diversity of solids and a fairly constant content of gas ($\sim$15–20 vol%). The complex shapes indicate slow evolution, with repeated fragmentation and modification of the original contents. There is a surprising diversity of solid phases present which can be classified into four groups (see also *Clocchiatti* et al., 1981):

(a) *Chlorides*

These make up about 50% of the whole mineral content. The most abundant species is NaCl, followed by KCl and Fe, Mg, Ca and Ni chlorides. Fe-rich chlorides may be suspected from their yellowish color and they seem to be almost as abundant as NaCl in some cases.

(b) *Carbonates*

These are present in most inclusions in relatively constant amounts (15–20% of the mineral content) and are invariably very Mg-rich, either magnesite or Mg-rich dolomite.

(c) *Sulfates*

Gypsum occurs sporadically and, if present, makes up at least 20% of the inclusion. But it seems to be absent in many inclusions, notably in the smallest ones (heterogeneous trapping).

(d) *Other Minerals*

This group comprises essentially silicates and opaques. Among the silicates talc is the most common, followed by clinochlore, cancrinite and serpentine. The opaques comprise iron oxides (hematite) and hydroxides (goethite), sometimes with significant quantities of Mn and Cr. The total content of all of these other minerals is also highly variable, from 0 to about 20% in volume.

Secondary inclusions, in most olivine crystals, are present in well developed trails (Fig. 9). The mineral content is much more homogeneous as compared to the primary inclusions and the relative proportions of chlorides and carbonates remain constant within a single trail. Secondary inclusions were trapped very rapidly and have experienced much less local evolution and modification than the primary inclusions.

The gas phase, analyzed by microthermometry and micro-Raman spectroscopy (Microdil 28, Free University, Amsterdam, E. A. J. Burke analyst), contains two species: CO_2 and/or N_2. The N_2/CO_2 ratios are highly variable, much more than reported by *Clocchiatti* et al., (1981) for gem peridot

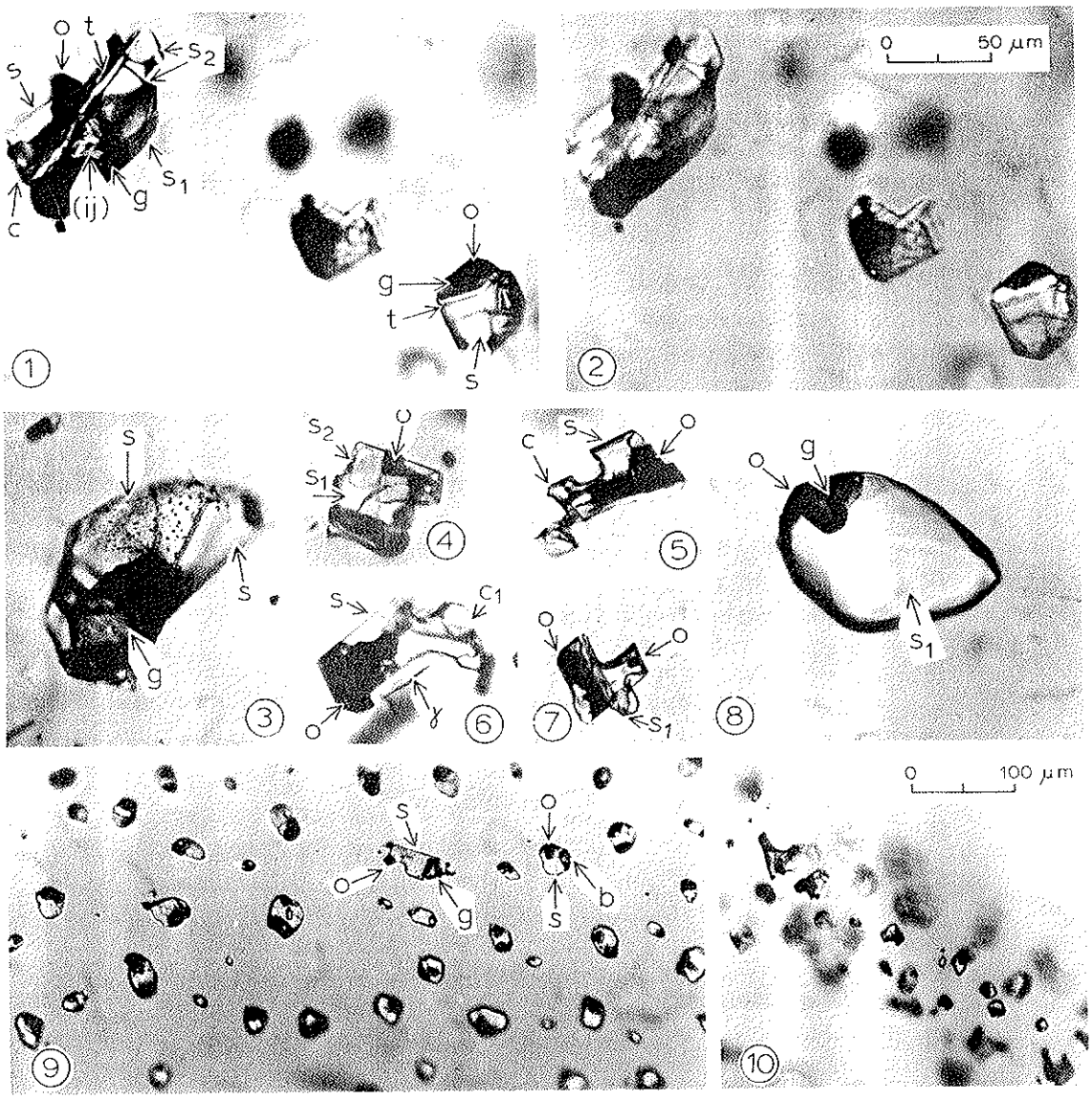

Fig. 9. Fluid inclusions in olivinite (Z-104) of Zabargad Island. In all inclusions, liquid (H_2O) is conspicuously absent at room temperature. Only gas (low density CO_2 and N_2) and a variety of solids (mostly chlorides) are present. Photos 1 to 8: primary inclusions (same scale, 1 and 2: same inclusions, 2: crossed nicols, all other photos: parallel nicols). Photos 9 and 10: secondary inclusions (same scale, 9: parallel to inclusion plane, 10: perpendicular to inclusion plane). Note for the primary inclusions the often irregular shape (4 to 7) and the variety of solids, which contrasts with the relative homogeneity of the secondary inclusion content. Symbols in all photographs: o = opaque (Fe or Cr oxide ?), s = undifferentiated chloride (in 3, with numerous gas bubbles at the surface), s_1 = halite, s_2 = iron chloride, c = undifferentiated carbonate, c_1 = magnesite, t = talk (Photo 1), γ = gypsum (Photo 6), (ij) = undifferentiated birefringent minerals (probably sulfates or silicates, Photo 1), g (and b, Photo 9) = squeezed gas bubble

from Zabargad (0.6–1.3). We have found, in fact, all intermediates between pure N_2 and pure CO_2. Relatively pure CO_2 appears to be the most abun-

dant species and apparently there are very few mixed fluids in the 50% range. Pure N_2 fluids may occur very close to pure CO_2, sometimes in the same trail of secondary inclusions. This suggests a very local mechanism controlling the gas composition. Microthermometric determinations of the temperature of phase transition are not easy to make, due to the small size of most inclusions and the irregular shape of the gas bubbles. Many inclusions remain gaseous ("empty") to the lowest temperature reached by the freezing stage (−190°C Model Chaixmeca, Free University, Amsterdam). Only homogenization temperatures could be recorded, and they were always gaseous (liquid/vapor to vapor); for CO_2, they are between +10°C and 31°C (critical), and for N_2 between −155 and 170°C (the values given by *Clocchiatti* et al., 1981, were 10 to 29.6°C and −159 to 170°C, respectively). These data correspond to low density fluids and are 0.47 (critical) to 0.14 g/cm^3 for CO_2, and much lower values of 0.08 to 0.04 g/cm^3 for N_2.

(2) *Orthopyroxenite and Clinopyroxenite*

Fluid inclusions in these vein rocks have features very similar to those of fluid inclusions in olivinites. The pyroxenes are generally deformed and sheared, displaying prominent traces of slip(?) planes. Portions of the crystals are totally recrystallized. In spite of the deformations, pyroxene contains abundant fluid inclusions and the quantity of gas which can be studied by microthermometry is greater than in olivine. The sizes of the inclusions vary from 2 to 15 μm and the shapes are prominently rectangular or elongated rectangular (negative crystals in pyroxene). The primary inclusions are isolated, similar to those in the olivinites, whereas the secondary inclusions occur in trails. Both types of inclusions were formed before deformation took place. Inclusions affected by the deformation were reequilibrated.

The nature of fluid inclusions in the pyroxenites (containing NaCl, carbonates and CO_2) are generally similar to those in the olivinite (Z-104), but differ significantly in detail. The mineral content is less (< 50% of the cavity) and less diverse: (a) Chlorides, dominated by NaCl, (b) Carbonates (Fig. 10), probably Fe-rich dolomite, and (c) sulfates have not been observed. Silicate minerals also seem to be absent, iron oxides, however, appear to be present.

A brown mineral was encountered, which has a strong broad line around 750 cm^{-1} in Raman spectra. This line is diagnostic of corundum or aluminates. It could indicate a phase exsolved from the high pressure pyroxene (Al-rich).

With regard to the gas phase, two major differences between that in the olivinites and pyroxenites may be noted: (a) No N_2 has been detected in significant amounts in pyroxenites, and (b) Most importantly, the CO_2 density in the pyroxenites is much higher than in the gem olivine. Most inclusions are biphased (liquid/gas) at room temperature and all homogenization occurs in the liquid by disappearance of the gas bubble. Homogenization temperatures are very constant, all measured values being between +26 and +30.9°C, with a distinct maximum at 30°C. This corresponds to densities of 0.698 g/cm^3 (T_h = 26°C) and trapping pressures of about 3 kb, for a reference temperature of 1000°C. These values, however, are minima, and due to the deformation of the pyroxene the densities may have significantly decreased; the initial values could have been much higher.

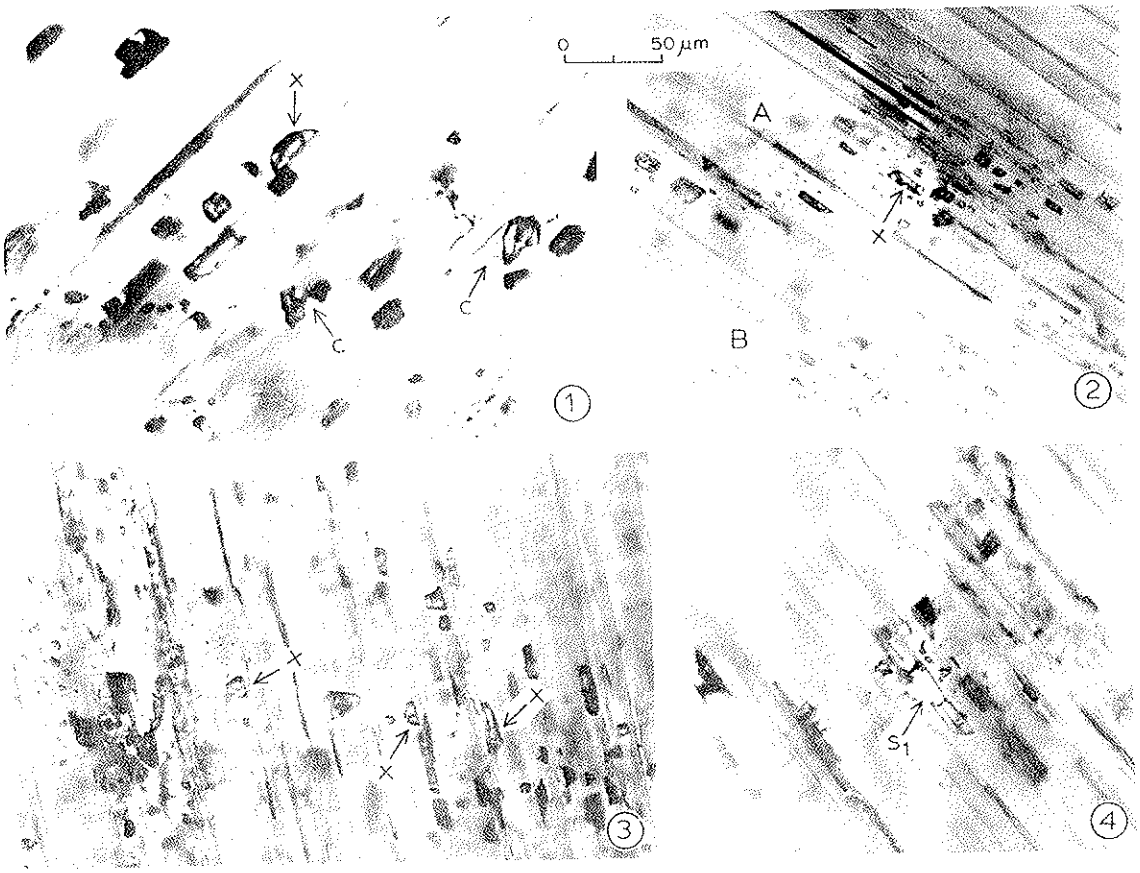

Fig. 10. Fluid inclusions in orthopyroxene Z-31 (all photos at same scale). Primary and secondary inclusions (A and B, Photo 2: trace of inclusion plane). The shape of nearly all inclusions is subrectangular, the length being parallel to the trace of the prominent slip plane (reorientation of former inclusions during deformation). X = 2-phase (liquid-vapor) CO_2 at room temperature, homogenization temperature (liquid) about 30°C (see text). c = undifferentiated carbonate, s_1 = halite

Discussion

(1) *Peridotites*

Petrological and mineralogical characteristics, as well as bulk rock and mineral compositions unambiguously indicate that the three peridotite bodies of Zabargad Island must originate from the sub-Red Sea upper mantle. In contrast to many other Alpine-type peridotites, and especially ophiolitic peridotites of the world, Zabargad peridotites seem to be more fertile and hence, closer to pristine mantle compositions. The pristine nature of these rocks has also been emphasized by earlier workers (*Bonatti* et al., 1986; *Piccardo* et al., 1988). On a plot of MgO versus the refractory elements Al, Ti, Sc and Yb Zabargad data lie very nicely on the best fit line defined by 20 spinel lherzolite xenoliths from occurrences on three continents (*Palme* and *Nickel*, 1985) (Fig. 11). Similar data of *Frey* et al. (1985) on the Ronda peridotites define exactly the same trends as those shown in Fig. 11. *Palme* and *Nickel* (1985) reported that the upper mantle has a Ca/Al ratio which

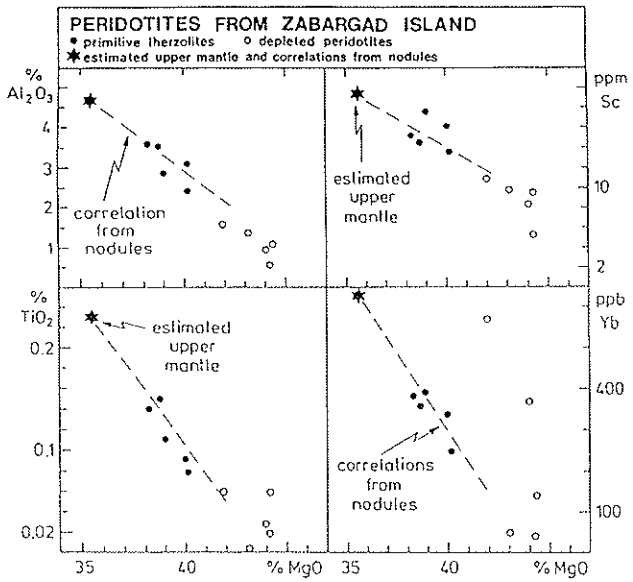

Fig. 11. MgO vs. refractory elements Al_2O_3, TiO_2, Sc and Yb for primitive and depleted peridotites of Zabargad Island, compared with upper mantle ultramafic xenoliths and the estimated upper mantle composition (*Palme* and *Nickel*, 1985). Note the deviation of some of the depleted peridotites from the fractionation trend — a consequence of metasomatic enrichment following the depletion event

is 15% higher than the cosmic ratio defined by undifferentiated meteorites. The Zabargad data presented here support these findings, with all fertile peridotite samples showing Ca/Al ratios clearly higher than the cosmic ratio of 1.10 (except for Z-14 which has a lower ratio, but shows metasomatic alteration by addition of Al-spinel).

The similarity in compositions of spinel lherzolite xenoliths and Zabargad peridotites is also evident in the trace element abundances. For example, the range in Ir contents of the Zabargad peridotites is typical of that for spinel lherzolite xenoliths (*Jagoutz* et al., 1979; *Kurat* et al., 1980; *Embey-Isztin* et al., 1989; *Spettel* et al., 1991). Ir/Au ratios of Zabargad peridotites are also within the range of typical upper mantle rocks. All Zabargad upper mantle samples for which data are available have higher absolute concentrations of Ir than Au, whereas basalts and crustal rocks always show the reverse. Other chemical similarities between Zabargad peridotites and xenoliths include the abundances of Mn, Cr, Co, Zn and Ga.

Metasomatic alteration is evident in peridotites containing large amphibole and/or clinopyroxene porphyroblasts (Z-17D, Z-36, Z-17G, Z-19). All of these rocks show strong enrichments in incompatible trace elements (LREE up to 55 × CI, HREE 2xCI) (Fig. 6B). These patterns are apparently dominated by the REE contents of the porphyroblasts, as is clearly evident from the pattern of the isolated amphibole Z-36A (Figs. 6B and 7A). According to the REE distribution coefficients between amphibole and liquid (e.g., *Irving*, 1978) the latter must have been very rich in REEs, especially in the LREEs. A similar fluid must have been responsible for the contamination of Z-17G and Z-19, rocks originally fairly strongly depleted in trace elements. A surprisingly large difference in the degree of metasomatic alteration shows up between Z-17G and Z-17D, two parts of the same rock, with one part (Z-17G) much less deformed and sheared than the other (Z-17D). It demonstrates, quantitatively, that tectonic processes can facilitate the percolation of fluids through pathways created by intensive shearing. Similar enrichment of LREEs and other

incompatible elements in deformed peridotite xenoliths have been described in a number of cases (e.g., Dreiser Weiher, Germany, *Stosch* and *Lugmair*, 1986; Kilbourne Hole, Arizona, *Bussod* and *Williams*, 1987; Transdanubian Volcanic Region, Hungary, *Kurat* et al., 1991a; *Downes* et al., 1992). Sr and Nd isotope ratios also have been shown to be heterogeneous on a scale of meters or less in Zabargad peridotites (*Brueckner* et al., 1988).

The halogen data give further evidence of the percolation of fluids into the tectonically sheared peridotites (Table 5). The Cl, Br, and I concentrations of metasomatized peridotite Z-17 and depleted peridotite Z-103 are factors of 10–100 times higher than the halogen contents of ultramafic xenoliths (*Jagoutz* et al., 1979). The highest enrichments found are for Cl. In MORBs the halogens behave as incompatible elements during partial melting and correlate with LREEs. The La/I ratio for MORBs and ultramafic nodules is about 160, whereas it is only 59 for the Z-17D (more sheared) and 9 for Z-17G (less sheared) peridotites, and 0.1 for Z-103 (depleted peridotite). Because of the strong I depletion of seawater, relative to Cl and Br, the I in Zabargad peridotites cannot be derived from seawater interaction. However, the seawater may have undergone a few changes before reaching the peridotite, or the water may be derived from the sediments. An alternative explanation may be that these element ratios are indicative of a saline fluid phase. According to the fluid inclusion data on vein rock minerals this fluid phase was very poor in water. Therefore, it is likely that the I has been derived directly from the upper mantle.

(2) *Vein Rocks*

Our data allow an in-depth discussion on the controversial origin of ultramafic and related vein rocks. Mono- and polymineralic ultramafic dikes and veins have for a long time been regarded as being of magmatic origin and attributed to processes such as partial melting, fractional or flow crystallization (e.g., *Boudier* and *Nicolas*, 1972; *Cawthorn*, 1975; *Frey*, 1980; *Wilshire* et al., 1991). The transformation of the original igneous textures to metamorphic textures has been discussed by *George* (1978).

On the other hand, the possibility of a hydrothermal generation of dunite and pyroxenite veins and layers was outlined as early as 1949 by *Bowen* and *Tuttle*. A similar origin has been suggested for hornblendites, pyroxenites and olivinites by a number of other workers (*Hess*, 1960; *Dungan* and *Avé Lallemant*, 1977; *Loomis* and *Gottschalk*, 1981; *Boudrean* et al., 1986; *Schiffries* and *Skinner*, 1987). Arguments in favour of a non-magmatic origin include structural and textural features such as the absence of cumulate textures, the continuity of very thin layers, monomineralic banding, the variety of juxtaposed layers of differing compositions and cross-cutting relationships (*Loomis* and *Gottschalk*, 1981), as well as chemical such as rock compositions that cannot be derived by known igneous processes.

Many of the textural and structural features noted above were observed in the Zabargad vein rocks. In addition, there is chemical evidence that the vein rocks cannot easily be reconciled with a magmatic origin. For example, the REE pattern of the cleanest gem peridot is such that, using the experimentally determined olivine/liquid distribution coefficients of *McKay* (1986) (Fig. 7B), a REE pattern for the liquid is indicated which is incompatible with a silicate melt. This liquid (taken

as an equivalent silicate liquid) must have had an Yb content of almost 10 × CI and very high LREE contents. Such a pattern is characteristic of CO_2-rich vapors in equilibrium with silicate melts (e.g., *Wendlandt* and *Harrison*, 1979). The high Cl and Br contents of vein rocks of Zabargad Island and the hypersaline, H_2O-free fluid inclusions in vein rock minerals make it very likely that the Zabargad ultramafic vein rocks are precipitates of high p-T fluids.

(3) *Thermobarometry*

Application of the single pyroxene thermobarometer (*Mercier*, 1980) reveals a surprisingly large range of p-T conditions recorded in the Zabargad rocks (Fig. 12). Bulk (rehomogenized) pyroxene compositions reflect, as expected, the highest p-T conditions of formation ranging up to 1280°C at 27 kb (Z-103G). Relics recording the highest p-T conditions are present exclusively in the pyroxenites and harzburgites (Z-103G, Z-30, Z-102, Z-51, Z-103H, Z-37) and the wehrlite Z-26.

A pronounced cluster, around 930–1000°C at 10–12 kb, consists mainly of rocks which apparently recorded a major recrystallization event in their porphyroclasts and exsolution lamellae. A second cluster is present at 900°C at 6 kb. This cluster comprises porphyroclasts and some neoblasts. The single pyroxene thermobaro-

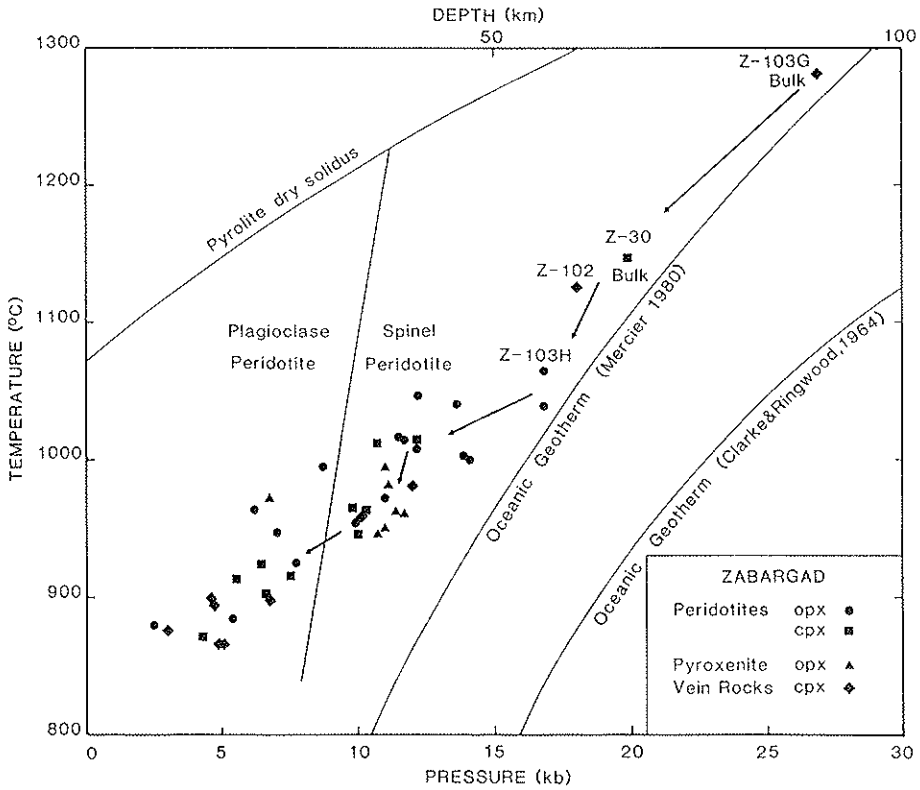

Fig. 12. Temperature-pressure plot for peridotites and pyroxenites of Zabargad Island, using the single pyroxene thermobarometry of *Mercier* (1980). The arrows trace the p-T path of the uprising peridotite from depth to the surface of the island. The oceanic geotherms of *Mercier* (1980) and *Clarke* and *Ringwood* (1964) are shown for comparison

meter of *Mercier* (1980) should not be applicable to that p-T regime but it reveals "acceptable" and reasonable conditions for some pyroxene compositions, however, not for all of them. Most neoblasts give unacceptably high pressure estimates (as expected). The temperature estimates were checked by the two-pyroxene thermometer of *Wells* (1977) and are comparable in most cases. The two-pyroxene thermometry revealed temperature estimates between 970 and 810°C (mylonite Z-106 and recrystallized peridotite Z-17D), respectively, with clusters around 870°C and 900–960°C, for the neoblasts and rims, in agreement with the single pyroxene thermometer.

The p-T development of the Zabargad peridotites directly reflects a fast uplift history as also indicated by other, independent observations (e.g., contact metamorphism, low degree of retrograde metamorphism). Relics representing the highest p-T conditions plot fairly close to the oceanic geotherm (*Mercier*, 1980). With increasing pressure release (uplift), the reequilibration conditions moved increasingly away from the geotherm towards higher temperatures. The difference between the geotherm and the Zabargad peridotites, at 10 kb, is about 180°C and apparently increases further with decreasing pressure. The slope of the p-T path indicates rapid ascent, which is supported by the small scale of plagioclase formation (see also *Bonatti* et al., 1986), and serpentinization in Zabargad peridotites. Extensive contact metamorphism of the Zabargad formation (hornfelses) and the lower crustal metamorphic rocks (*Boudier* et al., 1988) further supports the relatively rapid uplift of the Zabargad peridotites from the upper mantle.

Thermobarometry also convincingly demonstrates that the pyroxenitic vein rocks of Zabargad are of deep-seated origin. Apparently the clinopyroxenites record the highest p-T conditions. These data allow us to speculate on a sequence of vein rock formation (from highest p-T to lowest) which can eventually be verified by experimental studies: clinopyroxenites–orthopyroxenites–hornblendites–websterites–plagioclasites–olivinites.

Conclusions

The peridotites of Zabargad Island are of upper mantle origin. They are dominated by spinel and spinel-plagioclase lherzolites which are chemically fairly pristine and similar to fertile peridotite xenoliths in basalts. Zabargad peridotites differ, however, from common orogenic peridotites in their high proportion of fertile lherzolites.

Although fairly extensively and multiply recrystallized, Zabargad Island peridotites preserve some relic phase equilibria indicating derivation from great depth (>85 km). The p-T path of uplift coincides with the oceanic geotherm at greater depth but deviates successively from it towards higher T with falling p. This is interpreted as indicating rapid uplift, a view supported by the extensive contact metamorphism caused by the peridotites when they penetrated the lower crustal rocks, and especially the sediments of the Zabargad Formation, as well as by the low degree of retrograde metamorphism in the peridotites (*Moon*, 1923; *Kurat* et al., 1982a, b). The p-T path is interpreted as indicating two different modes of uprise: (1) An early diapiric stage, followed by (2) several tectonic stages. This is in accordance with structural (*Nicolas* et al., 1987) and geophysical data (*Styles* and *Gerdes*, 1983). The latter indicate extension of Zabargad peridotites to a depth of >8 km which means that the Zabargad peridotites are rooted in the upper mantle.

The less common depleted peridotite suite of Zabargad Island comprises mainly harzburgites and a few dunites. Beside having experienced depletion to varying degrees, they show addition of incompatible elements via metasomatism. The degree of metasomatism is highly variable and appears to be correlated with the degree of depletion, a feature also observed in upper mantle xenoliths (*Frey* and *Prinz*, 1978 and many subsequent workers). There are a few extreme examples of modal metasomatism (amphibole dunite Z-36 and Z-17D) and one sample (Z-17) which clearly demonstrates the importance of tectonization to facilitate metasomatism. Tectonization appears to be a prerequisite for metasomatism because it provides the necessary porosity and permeability.

Metasomatism is evident in a variety of different ways: (1) "Contamination" by incompatible elements (cryptic metasomatism) and (2) Formation of porphyroblasts, i.e., precipitation of amphibole, clinopyroxene, Al-spinel or plagioclase (patent metasomatism—compare *Dawson*, 1984). The fact that a variety of minerals formed (mostly one per rock) indicates that metasomatism took place under various p-T conditions from a variety of fluids. Metasomatism leading to the formation of clinopyroxene and amphibole porphyroblasts is always accompanied by the introduction of large amounts of incompatible trace elements into the rock (cf., Z-17, Z-26, Z-36, Z-19). This is, however, not the case with porhyroblasts of Al-spinel.

Precipitation from percolating fluids, rather than from silicate melts, is preferred here for the genesis of the monomineralic and pyroxenitic vein rocks. This type of vein rock formation has been extensively described and documented in the case of the Seiad Ultramafic Complex, California, by *Loomis* and *Gottschalk* (1981). As evidence, we can consider the hypersaline character of the abundant fluid inclusions and the dominance of CO_2 in these fluids. Trace element contents of all of the monomineralic rocks indicate high contents of incompatible elements and concentrations compatible with an origin from a CO_2-rich fluid phase according to the experimental data of *Wendlandt* and *Harrison* (1979). The character of the fluids is such that they must have been derived from peridotite reservoirs.

The nature of the occurrence of the monomineralic vein rocks reveals a close association of metasomatism with tectonic processes. The most impressive examples showing this relationship are the numerous occurrences of clinopyroxenites. They invariably occur in sheared peridotites which show a progressive growth of porphyroblasts of clinopyroxene from isolated grains, to stringers of grains, to veinlets and to veins (see also *Loomis* and *Gottschalk*, 1981). Clinopyroxene metasomatism and formation of clinopyroxenites must have taken place under high p-T conditions which allowed semiplastic flow of the peridotites. This view is supported by the high temperature relic equilibrium conditions preserved in some of the clinopyroxenites. Hornblendites seem to represent a transitional stage; some are associated with similar metasomatic alteration of the host rock, but some are not. Orthopyroxenites, olivinites, and plagioclasites are developed as clean veinlets and veins displaying no interaction with the wall rock. The wall rock apparently was brittle and tectonic strain did not result in plastic flow but in the opening of fissures. They were subsequently invaded by fluids which crystallized mainly a particular mineral. The opening of the fissures took place gradually under continuing movement. This is documented by the abundant relic phases of the host peridotite in the plagioclasites, and the tectonization and recrystallization omnipresent in the clinopyroxenites and orthopyroxenites.

Formation of vein rocks apparently took place in the upper mantle, probably in the asthenosphere (clinopyroxenites) and during uplift. The olivinites were possibly the latest veins formed, and the latest olivine within these rocks was the famous gem peridot. The whole sequence of vein rock formation apparently represents common and pervasive processes which may be active in the upper mantle during orogeny. Most vein rocks are monomineralic with the exception of plagioclasites and websterites. Websterites pose a problem needing further investigation. Trace element data indicate some relationship to the hornblendites, and this may provide a clue. As a working hypothesis we propose that the websterites may possibly represent former hornblendites which were exposed to conditions under which the amphibole broke down, released the water and recrystallized to an assemblage of clinopyroxene + orthopyroxene. All websterites display thoroughly recrystallized textures which obscure relic features.

Acknowledgements

We gratefully acknowledge the substantial help received from Eng. I. Kamel, Eng. K. El Marsy and Mr. F. Abdel Fattah, El Nasr Phosphate Company, Cairo, in organizing two expeditions to Zabargad Island in 1980 and 1986. Financial support was received from the Austrian "Fonds zur Förderung der wissenschaftlichen Forschung" (Project P4773, G. K., principal investigator) and the "Freunde des Naturhistorischen Museums in Wien". E. A. J. Burke is thanked for the Raman analyses. M. Prinz thanks Michael K. Weisberg for his help, and the project was partially supported by NASA Grant NAG 9–32.

References

Albee AL, Ray L (1970) Correction factors for electron probe micronalysis of silicates, oxides, carbonates, phosphates and sulfides. Anal Chem 42: 1408–1414

Bence AE, Albee AL (1968) Empirical correction factors for the electron microanalysis of silicates and oxides. J Geol 26: 382–403

Bonatti E, Hamlyn PR, Ottonello G (1981) The upper mantle beneath a young oceanic rift: peridotites from the Island of Zabargad (Red Sea). Geology 9: 474–479

Bonatti E, Clocchiatti R, Colantoni P, Gelmini R, Marinelli G, Ottonello G, Santacroce R, Taviani M, Abdel-Meguid AA, Assaf HS, El Tahir MA (1983) Zabargad (St. John's) Island: an uplifted fragment of sub-Red Sea lithosphere. J Geol Soc London 140: 677–690

Bonatti E, Ottonello G, Hamlyn PR (1986) Peridotites from the Island of Zabargad (St. John), Red Sea: petrology and geochemistry. J Geophys Res 91: 599–631

Boudier F, Nicolas A (1972) Fusion partielle gabbroique de la lherzolite de Lanzo. Schweiz Mineral Petrogr Mitt 52: 39–56

Boudier F, Nicolas A, Ji S, Kienast JR, Mevel C (1988) The gneiss of Zabargad Island: deep crust of a rift. Tectonophysics 150: 209–227

Boudreau AE, Mathez EA, McCallum IS (1986) Halogen geochemistry of the Stillwater and Bushveld Complexes: evidence for transport of the platinum-group elements by Cl-rich fluids. J Petrol 27: 967–986

Bowen NL, Tuttle OF (1949) The system MgO–SiO2–H2O. Geol Soc Am Bull 60: 439–460

Brueckner HK, Zindler A, Seyler M, Bonatti E (1988) Zabargad and the isotopic evolution of the sub-Red Sea mantle and crust. Tectonophysics 150: 163–176

Bussod G, Williams D (1987) Thermal evolution of the lower crust and upper mantle in the southern Rio Grande Rift. Terra Cognita 7: 604

Carella R, Scarpa I (1962) Geological results of exploration in Sudan by AGIP Mineraria. 4th Arab Petrol Congr, Beirut. 23p

Cawthorn RG (1975) The amphibole peridotite–metagabbro complex, Finero, northern Italy. J Geol 8: 437–457

Clarke SP, Ringwood AE (1964) Density distribution and constitution of the mantle. Rev Geophys 2: 35–88

Clocchiatti R, Massare D, Jehanno C (1981) Origine hydrothermale des olivines gemmes de l'ile de Zabargad (St. John's) Mer Rouge, par l'etude de leurs inclusions. Bull Mineral 104: 354–360

Dawson JB (1984) Contrasting types of upper-mantle metasomatism? In: Kornprobst J (ed) Kimberlites II. The mantle and crust-mantle relationships. Elsevier, Amsterdam, pp 289–294

Downes H, Embey-Isztin A, Thirlwall MF (1992) Petrology and geochemistry of spinel peridotite xenoliths from the western Pannonian Basin (Hungary): evidence for an association between enrichment and texture in the upper mantle. Contrib Mineral Petrol 109: 340–354

Dreibus G, Spettel B, Wänke H (1979) Halogens in meteorites and their primordial abundances. In: Ahrens LH (ed) Origin and Distribution of the Elements. Pergamon Press, Oxford New York, pp 33–38

Dungan MA, Ave-Lallemant HG (1977) Formation of small dunite bodies by metasomatic transformation of harzburgite in the Canyon Mountain ophiolite, northeast Oregon. In: Dick HJB (ed) Magma Genesis. Oregon Dept Geol Mineral Res Bull, pp 109–128

El Shazly EM, Saleeb GS (1972) Scapolite-cancrinite mineral association in St. John's Island, Egypt. XXIV Internat Geol Congr, Montreal, Sect 14: 192–199

El Shazly EM, Saleeb-Roufaiel GS (1979) Genesis of peridotite in St. John's Island, Red Sea, and its relation to the metasomatism of the ultrabasic rocks. Egypt J Geol 22: 103–122

El Shazly EM, Saleeb-Roufaiel GS, Zaki N (1974) Quaternary basalt in Saint John's Island, Red Sea, Egypt. Egypt J Geol 18: 137–148

Embey-Isztin A, Scharbert HG, Dietrich H, Poulditis H (1989) Petrology and geochemistry of peridotite xenoliths in alkali basalts from the Transdanubian Volcanic Region, West Hungary. J Petrol 30: 79–105

Frey FA (1980) The origin of pyroxenites and garnet pyroxenites from Salt Lake Crater, Oahu, Hawaii: Trace element evidence. Am J Sci 280-A: 427–449

Frey FA, Prinz M (1978) Ultramafic inclusions from San Carlos, Arizona: petrologic and geochemical data bearing on their petrogenesis. Earth Planet Sci Lett 38: 129–176

Frey FA, Suen CJ, Stockman HW (1985) The Ronda high temperature peridotite: geochemistry and petrogenesis. Geochim Cosmochim Acta 49: 2469–2491

George RP (1978) Structural petrology of the Olympus ultramafic complex in Troodos ophiolite, Cyprus. Geol Soc Am Bull 89: 845– 865

Girdler RW, Styles P (1974) Two stage Red Sea floor spreading. Nature 247: 7–11

Hess HH (1960) Stillwater igneous complex, Montana: a quantitative mineralogical study. Geol Soc Am Mem 80: 230 pp

Irving AJ (1978) A review of experimental studies of crystal/liquid trace element partitioning. Geochim Cosmochim Acta 42: 743–770

Jagoutz E, Palme H, Baddenhausen H, Blum K, Cendales M, Dreibus G, Spettel B, Lorenz V, Wänke H (1979) The abundances of major, minor and trace elements in the earth's mantle as derived from primitive ultramafic nodules. Proc Lunar Planet Sci Conf 10th: 2031–2050

Kruse H (1979) Spectra processing with computer graphics. Proc Am Nucl Soc Top Conf, Mayaguez, Puerto Rico, DOE Conf.-78421: 76–84

Kurat G (1991) Geologie und Geochemie der Insel Zabargad (Ägypten, Rotes Meer). Wiss Film (Wien) 42: 134–142

Kurat G (1992) Geologie und Geochemie der Insel Zabargad (Ägypten, Rotes Meer). Mitt Österr Mineral Ges 137: 89–98

Kurat G, Palme H, Spettel B, Baddenhausen H, Hofmeister H, Palme C, Wänke H (1980) Geochemistry of ultramafic xenoliths from Kapfenstein, Austria: evidence for a variety of upper mantle processes. Geochim Cosmochim Acta 44: 45–60

Kurat G, Niedermayr G, Prinz M, Brandstätter F (1982a) High temperature peridotite intrusion into an evaporite sequence, Zabargad, Egypt. Terra Cognita 2: 240

Kurat G, Niedermayr G, Prinz M (1982b) Peridot von Zabargad, Rotes Meer. Der Aufschluss 33: 169–182

Kurat G, Brandstätter F, Palme H, Spettel B, Prinz M, Touret J (1983) Mobilizations in upper mantle rocks from Zabargad, Red Sea. Terra Cognita 3: 125

Kurat G, Ntaflos T, Brandstätter F, Palme H, Spettel B, Prinz M, Touret J (1984) Metasomatism of the upper mantle rocks from Zabargad Island, Red Sea. XXVII Internat. Geol. Congr., Abstracts V, Sect. 10, 11, Moscow: 324–325

Kurat G, Ntaflos T, Palme H, Dreibus G, Spettel B, Prinz M, Touret J (1985) Upper mantle vein pyroxenites: evidence for nonmagmatic origin. Terra Cognita 5: 439–440

Kurat G, Embey-Isztin A, Kracher A, Scharbert H-G (1991a) The upper mantle beneath Kapfenstein and the Transdanubian Volcanic Region, E Austria and W Hungary: a comparison. Mineral Petrol 44: 21–38

Kurat G, Ntaflos T, Kerschner H (1991b) Geologie und Geochemie der Insel Zabargad. Eur J Mineral , Beih 3/1: 160

Loomis TP, Gottschalk RR (1981) Hydrothermal origin of mafic layers in alpine-type peridotites: evidence from the Seiad Ultramafic Complex, California, USA. Contrib Min Petrol 76: 1–11

McKay GA (1986) Crystal/liquid partitioning of REE in basaltic systems: extreme fractionation of REE in olivine. Geochim Cosmochim Acta 50: 69–79

Mercier J-CC (1980) Single-pyroxene thermobarometry. Tectonophysics 70: 1–37

Mercier J-CC, Nicolas A (1975) Textures and fabrics of upper-mantle peridotites as illustrated by xenoliths from basalts. J Petrol 16: 454–487

Moon FW (1923) Preliminary geological report on St. John's Island, Red Sea. Geolog Surv Egypt, Cairo, Egypt. 36pp

Moon FW (1925) A preliminary note on the rocks of St. Johns Island in the Red Sea. CR XIIIe Congr. geolog. internat. 1922, Viallant-Carmanne, Liege: 1001–1004

Nicolas A, Boudier F, Lyberis N, Montigny R, Guennoc P (1985) Zabargad (Saint-John) Island: a key-witness of early rifting in the Red Sea. CR Acad Sc Paris II: 1063–1068

Nicolas A, Boudier F, Montigny R (1987) Structure of Zabargad Island and early rifting of the Red Sea. J Geophys Res 92: 461–474

Ntaflos T, Brandstätter F, Kurat G (1984) Petrologie der Ultramafitite von Zabargad, Rotes Meer. Fortschr Mineral, Bh 1 62: 174–176

Oberli R, Ntaflos T, Meier M, Kurat G (1987) Emplacement age of the peridotites from Zabargad Island (Red Sea): a zircon U-Pb isotope study. Terra Cognita 7: 334

Palme H, Nickel KG (1985) Ca/Al ratio and composition of the Earth's upper mantle. Geochim Cosmochim Acta 49: 2123–2132

Palme H, Suess HE, Zeh HD (1981) Abundances of the elements in the solar system. In: Scheifers K, Voigt HH (eds) Landoldt-Boernstein. Springer, Berlin Heidelberg New York, pp 257–273.

Petrini R, Joron JL, Ottonello G, Bonatti E, Seyler M (1988) Basaltic dykes from Zabargad Island, Red Sea: petrology and geochemistry. Tectonophysics 150: 229–248

Piccardo GB, Messiga B, Vannucci R (1988) The Zabargad peridotite-pyroxenite association: petrological constraints on its evolution. Tectonophysics 150: 135–162

Pott PE (1898) Expedition S. M. Schiff "Pola" in das Rothe Meer Bd. I Nördliche Hälfte,

Beschreibender Theil. Berichte der Commission für Oceanographische Forschungen K. Hof- und Staatsdruck. Wien 1–18

Schiffries CM, Skinner BJ (1987) The Bushveld hydrothermal system: field and petrologic evidence. Am J Sci 287: 566–595

Seyler M, Bonatti E (1988) Petrology of a gneiss-amphibolite lower crustal unit from Zabargad Island, Red Sea. Tectonophysics 150: 177–207

Spettel B, Palme H, Ionov DA, Kogarko LN (1991) Variations in the iridium content of the upper mantle of the Earth. Lunar Planet Sci 22: 1301–1302

Stosch H-G (1982) Rare earth element partitioning between minerals from anhydrous spinel peridotite xenoliths. Geochim Cosmochim Acta 46: 793–811

Stosch H-G, Lugmair GW (1986) Trace element and Sr and Nd isotope geochemistry of peridotite xenoliths from the Eifel (West Germany) and their bearing on the evolution of the subcontinental lithosphere. Earth Planet Sci Lett 80: 281–298

Styles P, Gerdes KD (1983) St.John's Island (Red Sea): a new geophysical model and its implications for the emplacement of ultramafic rocks in fracture zones and at continental margins. Earth Planet Sci Lett 65: 353–368

Triulzi AE (1898) Expedition S. M. Schiff "Pola" in das Rothe Meer, nördliche Hälfte. Wissenschaftliche Ergebnisse 11. Relative Schwerebestimmungen. Denkschr K Akad Wiss Wien Math-naturw Kl 65: 131–206

Wasson JT (1985) Meteorites. Their Record of Early Solar-System History. WH Freeman, New York, 267pp

Wedepohl KH (ed) (1969) Handbook of Geochemistry. Springer, Berlin Heidelberg New York, 6 vols

Wells PRA (1977) Pyroxene thermometry in simple and complex systems. Contrib Mineral Petrol 62: 129–139

Wendlandt R, Harrison WJ (1979) Rare earth partitioning between immiscible carbonate and silicate liquids and CO2 vapor: results and implications for the formation of light rare earth-enriched rocks. Contrib Mineral Petrol 69: 409–419

Wilshire HG, McGuire AV, Noller JS, Turrin BD (1991) Petrology of lower crustal and upper mantle xenoliths from the Cima volcanic field, California. J Petrol 32: 169–200

Zipfel J, Palme H, Specht S, Kurat G (1991) Ca-Zonierung in Olivinen des Zabargad Peridotites: Hinweise auf eine langsame Abkühlung. Eur J Mineral, Bh 3/1: 309

Authors' addresses: Prof. Dr. *G. Kurat* and *Dr. F. Brandstätter*, Naturhistorisches Museum, Burgring 7, A-1010 Wien, Austria; Dr. H. Palme, Dr. B. Spettel, Dr. C. Palme, Dr. G. Dreibus, Max-Planck-Institut für Chemie, Saarstrasse 23, D-N55122 Mainz, Federal Republic of Germany; Dr. A. Embey-Isztin, Termeszettudomanyi Muzeum, Muzeum Krt. 14-16, H-1088 Budapest, Hungary; Prof. Dr. J. Touret, Instituut voor Aardwetenschappen, Vrije Universiteit, NL-1081 HV Amsterdam, The Netherlands; Dr. T. Ntaflos, Institut für Petrologie, Universität Wien, Dr. Karl Lueger Ring 1, A-1010 Wien, Austria; and Dr. M. Prinz, Department of Mineral Sciences, American Museum of Natural History, New York, NY 10024, USA